# The Effect of Trimming Process Parameters and Strategies on the Trimmed Edge Quality of 6DR1 Aluminum

**by**

**Ke Wang**

**A thesis submitted in partial fulfillment**
**of the requirements for the degree of**
**Master of Science in Engineering**
**(Industrial and Systems Engineering)**
**in the University of Michigan-Dearborn**
**2019**

**Master's Thesis Committee:**

**Professor Ghassan Kridli, Chair**
**Assistant Professor Georges Ayoub**
**Andrey Ilinich, Ford Motor Company**
**George Luckey, Ford Motor Company**

# ACKNOWLEDGEMENTS

I would first like to thank my thesis co-advisors Professors Ghassan Kridli and Georges Ayoub of the College of Engineering and Computer Science at the University of Michigan Dearborn. The door to Profs. Kridli and Ayoub was always open whenever I ran into trouble with understanding experimental results or I needed guidance with organizing my thought in writing. They steered me in the right the direction whenever they thought I needed it.

I would also like to thank Drs. Andrey Ilinich and George Luckey at Ford Motor Company. I am grateful for their guidance and continuous support during my two years spent with them. They made my master thesis work enjoyable, and their comments and suggestions helped grow my perspective on how to conduct experiments and analyze them, thanks to you.

A special thanks to my family. I would like to thank my beloved wife, Xue Liang, thank you for your continuous support and for everything. Words can't express how grateful I am to my parents and parents in law for their support and all the sacrifices they made for me.

# TABLE OF CONTENTS

# LIST OF FIGURES

# LIST OF TABLES

# ABSTRACT

The purpose of this work is to investigate the trimmed edge stretchability of 6DR1 aluminum under multiple process conditions and strategies. The effect of four trimming parameters on the trimmed edge quality is studied namely; clearance, offal support, lower tool sharpness and upper tool sharpness. The upper and lower tools were micro-machined using a diamond tool and their corresponding sharpness were measured by 3D microscope to increase the study validation and reliability. Furthermore, three trimming strategies are investigated in this study namely; low temperature trimming, multiple-stage trimming, and upper tool shearing rake angles. In this study, the trimming is conducted along the transverse to the rolling direction (TD). Electro discharge machined (EDM) half dog-bone specimens are trimmed with various conditions and strategies. The trimmed edge stretchability is assessed either by measuring the total elongation or the local strain of the tensile tested trimmed specimens. A multiple linear regression analysis correlating trimming process and edge stretchability is used to determine the most significant trimming parameters. The regression model is used to determine the optimal trimming condition that results into high edge stretchability. Clearance between upper tool and lower tool is found to be the most significant trimming parameter that impacted the most the edge stretchability. For high support, the edge stretchability is less sensitive to the upper tool sharpness. For no support, the edge stretchability is sensitive to the upper tool sharpness with a negative linear relationship. At 10% clearance, the standard deviation of elongation increased with upper tool radius. A statistical method is used to investigate the effect of three trimming strategies on the edge stretchability. Based on the one-way ANOVA table, the multiple-stage trimming and low temperature trimming had no influence on the edge stretchability with 30% clearance.

# Chapter 1: Introduction

The use of Existing manufacturing processes is challenged by the significant increase in the utilization of light weight metals, specifically aluminum alloys, in the automotive industry driven by the need to produce fuel-efficient vehicles. One of widely used manufacturing processes by the auto industry is the shearing process. A variety of shearing technologies which process the metal for the following stamping process by cutting the stock without the formation of chips are used by the sheet metal industry. The shearing in automotive industry consist of blanking, piercing, and trimming. The tooling and processes are the same between the blanking and piercing, only the terminology is different: in blanking the punched out piece is used and called a blank; in piercing the punched out piece is scrap[1]. In contrast to the stamping and bending process in order to get plastic deformation, these operations lead to the total rupture of the metal[2]. To avoid confusion in terminology throughout this paper, unless given appropriate distinction, the use of trimming remains in context of traditional blanking operations. The trimming process is part of using curved cutting blade. Compared to other cutting method, such as laser cutting and water jet, the trimming process is extensively used by the automotive industry driven by speed and cost advantages[3] . The sheared edge quality resulting from the trimming process directly influences the strechability and flangeability of the sheared aluminum sheet under stamping. The study of the edge stretch help to determine the optimal trimming conditions maximizing the edge stretchability in the following automotive stamping processes. Under trimming conditions, the material fractures under a complex combination of plastic deformation and ductile fracture[4]. The lack of comprehensive understanding of the relationship between important trimming parameters and stamping edge stretchability motivates this study. In this work, the effect of trimming parameters and multiple trimming strategies on the edge quality is investigated using experimental and statistical approach. An illustration of the trimming process is presented in

figure 1.1(a). The blank is clamped between the lower tool and the pad with a constant clamping force. The upper tool is slightly offset from the lower tool; the offset is referred to as clearance. When the upper tool is in contact with the blank, a localized plastic area between the blade edges of the upper and the lower tool is formed that results into fracture. The trimming experiments are performed on a phi Pasadena hydraulic press. The trimming die is shown in Figure 1.1(b). Variable upper and lower trimming inserts can be used with the trimming die. Shims are placed behind the lower trim tool to control trimming clearance between the upper and lower trim tools.

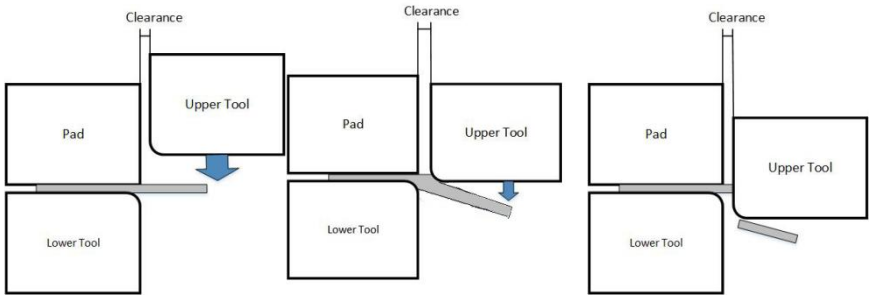


(a)

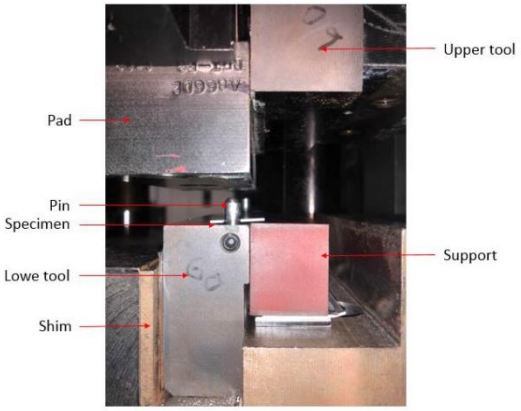


(b)

Figure 1.1: (a) Schematic representation of the trimming process (b) Trimming machine side view

The trimming process inducing damage and plasticity have a significantly impact on the edge stretchability in the following stamping process. The trimmed edge quality varies with trimming parameters such as clearance (the distance between upper tool and lower tool), upper and lower tools edge geometry, cutting angle and scrap support etc. (figure 1.2(a)) and special

trimming strategies such as the multiple-stage and low temperature trimming. For instance, the edge stretchability decreases from 15% nominal major strain to 4% when using trimming conditions that induce high damage and plastic deformation. In practical, the tool craftsmanship and flexibility make it difficult to control the optimal clearance while monitoring the wear in the tool cutting edge is difficult. For example, a partially trimmed automotive blank is shown in figure 1.2(b). Rectangular samples along the trimming line were taken out and metallographically investigated. A large clearance range from 0% to 40% and inconsistent upper tool and lower tool geometry projection were measured as shown in figure 1.2(b) and 1.2(c). One of the motivations of this study is to investigate the relationship between trimming parameters' variation and edge stretchability. The emphasis was made on optimization of the trimming conditions for a better edge stretch performance.

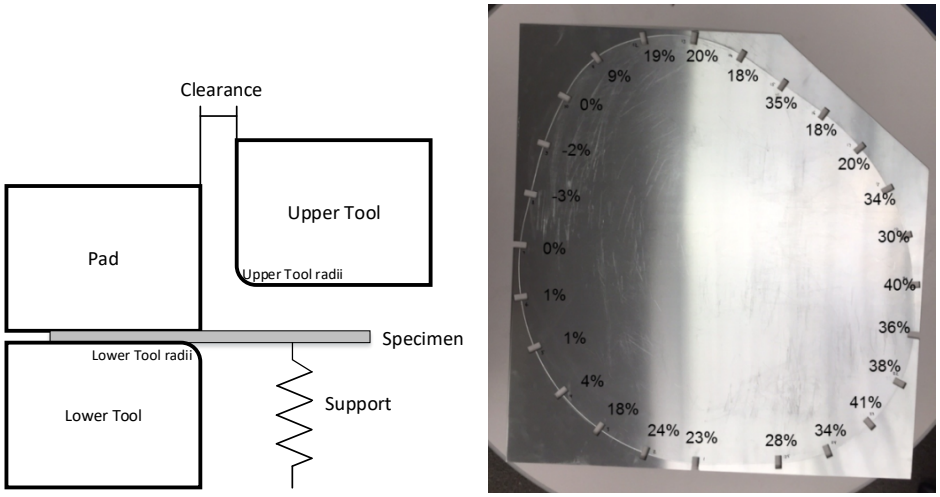


(a) (b)

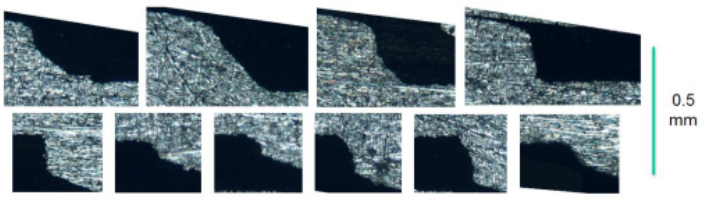


(c)

Figure 1.2: (a) Mainly trimming parameters (b) Partly trimmed close loop plate

(c) Tools geometry projection in the partly trimmed plate

Multiple trimming strategies were proposed in the literature to increase the sheared edge quality and stretchability . Hua-Chu Shih and Ming F. Shi [5] detected a proper upper tool geometry to improve the advanced high strength steel(AHSS) edge stretchability and figured out that the traditional zero degree trimming process lead to worse edge stretchability for AHSS. Authors of another paper proposed a multiple-stage punching process which reduced the degree and depth of hardening and eliminated the macroscopic damage of AHSS[6].

Within multiple methodologies of the trimming study, such as empirical, analytical, and numerical methods, the empirical method is utilized to investigate the trimming sheet metal. Two common experimental tests, hole expansion test i.e. HET (circumferential trimming followed by a hole expansion operation) and half-dog bone tensile test (straight-line trimming followed by a tensile test), are developed as standard methods for determining edge stretch. This study utilizes the half-dog bone test. The specimen's geometry used in this study is presented in figure 1.3. In general, three discrete specimen rolling directions, longitudinal direction (LD), diagonal direction (DD), and transverse direction(TD) (figure 1.4), are defined by trimming action relative to the grain direction of the specimens. In this study, only the TD is selected as the worst case with the lowest edge stretchability. The design of the specimen geometry is inspired from the ASTM E8 standards to localize the deformation and guarantee a fracture in the gauge area. The material used in this study is a 6DR1 series aluminum sheet of 0.9 mm thickness widely used for stamping outer vehicle body panels.

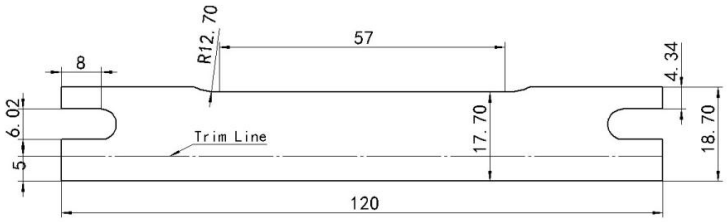


Figure 1.3: Geometry of the half-dog bone specimen, dimensions in mm

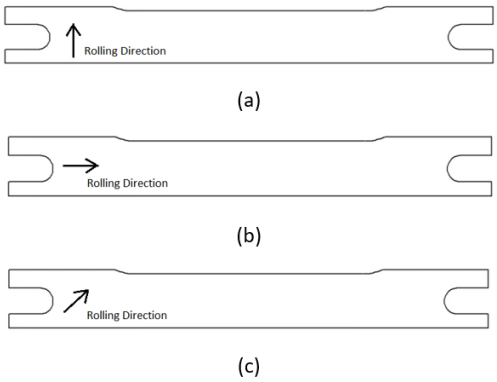


Figure 1.4: Trim line orientation relative to rolling direction of sheet material (a) Transverse direction “T”, trim line 90° to rolling direction; (b) Longitudinal “L” direction, trim line 0° to rolling direction; (c) Diagonal “D”, trim line 45° to rolling direction

Investigating the failure mechanisms of a trimmed sheet of metal is essential for improving structural properties in stamping operations. To understand the induced damage under trimming conditions, the deformation mechanisms controlling the shearing process should be inspected. After the tools are in contact with the metallic sheet a region of intense shear stress develops, referred to as the plastic zone, and is accompanied with bending caused by the offset loading, that will ultimately lead to failure. The extent of the plastic zone depends on the materials properties and the trimming process parameters[7], [8]. Therefore, the shear edge quality depends on the extent of the plastic zone and hence the trimming process parameters, such as clearance, upper and lower tools edge geometry, cutting angle and sliver support etc. The fundamental shear edge geometry can be characterized with five typical geometrical features (rollover, burnish, fracture, burr and roughness) as shown in figure 1.5. Studying the evolution of the shear edge geometrical features helps estimate the extent of the plastic zone, the induced damage and therefore provide an efficient trimming process optimization tool. The formation of the shear edge geometrical features is depicted in four distinctive stages: (1) rollover is formed by bending of the blank resulting from the contact of the blank with the upper tool. (2) while the upper tool continue its movement downward, a high shear deformation zone is formed resulting in a smooth and flat area named burnish in the sheared edge. (3) As the upper tool continues its movement, two cracks initiate from the edge of the upper and lower tools

propagate and meet forming a rough area named fracture. (4) For some trimming conditions where the material flow significantly, the burr zone is formed.

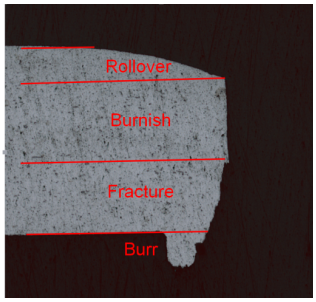


(a)

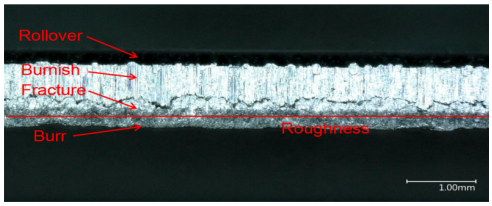


(b)

Figure 1.5: (a) Side view of trimmed edge (b) Front view of trimmed edge

The trimming process induces a large amount of geometrical imperfection and damaging plastic deformation along the material sheared edge. The extent of damage resulting from plastic deformation detected by metallographic cross-sectional images depends on the trimming conditions. For example, the optimal trimming condition results in smaller burr sizes and in general cleaner sheared edges with less plastic deformation, as shown in figure 1.6(a), and have higher edge stretch-ability. On the other hand, the less ideal trimming conditions leads to larger burr sizes and high plastic deformation in the sheared edge, as shown in Figure 1.6(b), resulting in reduced edge stretchability.

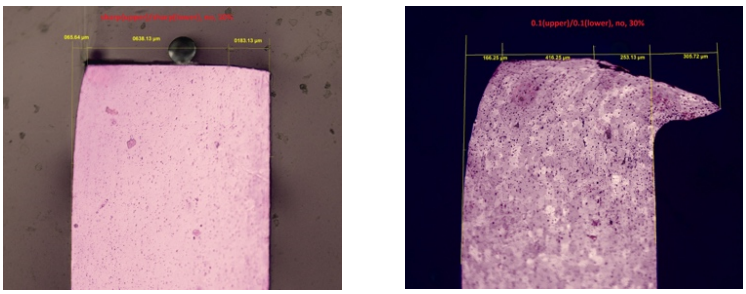

(a) (b)

Figure 1.6: (a) Less plasticity edge geometries under optimal trimming condition (b) Large plasticity edge geometries under unideal trimming condition

The clearance is the distance between the upper and lower trim tools. The clearance is usually reported as the percentage ratio between the distance separating the trim tools and the materials thickness. Clearance between the trim tools controls the extent of plastic deformation (plastic zone). Hence, increasing the clearance induces an increase in the size of the plastic zone and therefore more burr will be observed [9]. X. Hu et al. [10] reported that burr appears in conventional trimming conditions when the clearance is above 20% and consequently contribute to the decrease in edge stretch response. Golovashchenko and Ilinich [11] studied the mechanisms of burr generation and their influence on advanced high strength steel (AHSS) stretchability. The authors reported that higher clearance results into a decrease in the formability in stretch flanging. A design of experiment (DOE) base analysis was used by Hambli [12] to optimize the clearance that minimize blanking force, reduce tool wear and maximize sheared edge quality. Faura et al. [13] used finite element modeling (FEM) coupled with the Crockroft and Latham fracture criterion to optimize the clearance of an AISI 304 sheet. The authors report a good agreement between the experimental and numerical results. Golovashchenko[14][15] used elasto-plastic FEM model in plane strain formulation to analyze the effect of clearance on the formation of burr. Hu et al. [16] implemented numerical simulations on the trimmed edge stretchability of aluminum and showed that small clearance led to shear type failure and larger elongation, whereas large clearance led to splitting type failure and smaller elongation.

The effect of cutting angle on edge quality was investigated by Li [17] showing that at appropriate cutting angle the surface quality became insensitive to the blade sharpness, and almost zero burrs were produced for large clearances and extremely dull blades. The cutting angle determined the shear stress and normal stress components on the cut surface. A zero degree cut resulted in the least amount of normal stress (zero at the initial stage of cutting), and the normal stress component increased as the cutting angle increases[18]. The paper by Golovashchenko[19] showed that slivers still occurred with trimming angles in a production environment and often cutting angle was dictated by part geometry, therefore applying trimming angles could add die complexity and cost. Shih and Ming[3], [5] put forward a beveled shearing process where the tools with different combination of 3 angles are used to trim the specimens. The proper combination of angles leads to the reduction of the shearing force and energy and the improvement of part edge stretch by tensile and half dome test.

The effect of tool radius on edge quality was studied by Li [20]. The author reported that burr height increases with increasing tool radius. Moreover, the authors discussed the influence of tool radius on the blanking force and the effect on the sheared edge geometry. Golovashchenko[21] experimentally investigated the effect of evolving tool radius on the stretching performance and on eliminating slivers. It was suggested to machine a small radius on the upper tool and to limit the clearance to several percent of the material thickness. Wang et al.[8] used a two-step phenomenological Pre-Damage Mapping Mode (PDMM)l and a simplified PDMM model for the prediction of the sheared edge of a hole blanked AHSS. It was reported that tool wear increases considerably residual damage in the shear affected zone.

Golovashchenko[19] reported that in conventional trimming conditions cracks initiate and propagate in the aluminum blank from both the upper and lower shearing edges for clearances less than 20%. However, cracks are more developed at the upper shearing edge. Furthermore, for clearances above 20% cracks initiate and propagate only from the upper shearing edge. The author attributed those observations to the bending of the offal that changes the symmetry of the shearing process by adding tensile stresses to the upper edge and compression stresses to the lower edge. Hence Golovashchenko [19] proposed a modification to the conventional trimming process, in which a supporting force on the offal is added to reduce the offal rotation.

The authors demonstrated that bending is eliminated by adding mechanical support to the offal, which resulted into reducing burr size and eliminating slivers. Furthermore, Golovashchenko and Ilinich [11] reported that with the clearances between 20%-40%, the modified trimming condition produces smaller burrs than conventional trimming condition. Furthermore, the stretchability of trimmed aluminum sheets in modified trimming condition is reported to be larger than in conventional trimming condition. However, for smaller clearances, the difference between the stretchability of trimmed aluminum sheets with modified and conventional trimming conditions are statistically insignificant. Later, Golovashchenko and Ilinich [22] and Hu[16] investigated the fracture mechanisms and burr reduction in the modified trimming condition using experimental method and numerical simulations. It is reported that an inherent axisymmetric membrane constraint acts to resist offal rotation, and therefore, reduces the onset of burrs.

Burrs are geometrical imperfections in the sheared edge resulting from the material's plastic flow. Burrs may create difficulties in stamping operations. The burrs are the major source of early fracture when stretching is applied along the sheared edge. Hence, eliminating burr in the blanking process is important for edge quality improvement. Golovashchenko and Ilinich [11] showed that increasing clearance results into an increase of the burr size. Li[20] investigated experimentally the possibility of elimination burs by combining cutting angle and clearance. The burr height is very sensitive to trimming parameters and a deviation from optimal cutting conditions would result into an increase of the burr height. Golovashchenko[19][23] used numerical analysis to investigated the mechanisms of burr generation in conventional trimming. The author studied the effect of burr height on the fracture. Le et al.[24] presented an extensive experimental trimming study performed on aluminum alloy to demonstrated the effects of cutting clearance on the sheared edge quality. The authors concluded that the stretchability decreased with increasing burr size. Wang and Golovashchenko[25] investigated aluminum blanks sheared edge mechanisms of fracture subjected to shearing and stretching. It is reported that when stretching the sheared edge, small cracks initiate at the burr tip and propagate perpendicular to the sheared surface leading to early fracture.

The rollover is the top rounded zone induced by compressing the blank by the upper tool. Suliman[26] experimentally investigated the evolution of the sheared edge geometry with trimming parameters and concluded that the rollover increases with increasing clearance. Hilditch and Hodgson[27] compared the rollover depth of different materials and found that the rollover of steel increase with increasing clearance faster than rollover developed for Al and Mg. The different rollover depth mainly comes from the different ductility and work hardening of those material. By FEM-simulation, the maximum horizontal plastic depth is located in rollover[28].

The analytical method provides an excellent method to predict blanking force, strain in material and fracture mechanism. Initially the simple shear model was put forward by Atkin [23]. The authors investigated the effect of the trimming parameters on the maximum blanking load. Atkin made a conclusion that with clearance increasing, the peak load decreased and the punch penetration increased. The greater the material strain hardening exponent, the greater the maximum punch displacement and sheared zone width. Siekirk et al.,[24] built a model, which used regression analysis to determine the total strains, to predict the size of edge cracks based on the parameter of trimming. Based on the model, the optimum clearance value was found to get the minimum edge crack value. Qing Zhou[25] made a tension zone model to predict the plastic resistance and the plastic work in blanking and tearing of ductile metal plates. They found that the plastic resistance and the plasticity came from large rotation of material elements in the shear zone, and the reduction of shear area caused by the crack propagation through the thickness. The Blanking Model with a moving fracture front was proposed to predict the shear force, the plastic work, and the shape and size of the plastic shear zone. Based on a combination between the theory of cumulative damages, the model of the fractured element and the numerical solution of solid mechanics equations for elasto-plastic flow, Golovashchencko[26] proposed an approach to predict the quality of the sheared surface and elaborate the mechanism of the blank fracture. Slip line theory based on plane strain, rate-independent, rigid- perfectly plastic assumptions outlined by Johnson[27] showed an analytical approach to calculate shearing loads.

The numerical finite element methods are used to simulate the trimming process and predict the edge geometry as the empirical approaches often fail for some application involving high accuracy geometry specification, or non-standard materials and product shapes. The difficulty mainly comes from excessive element distortion resulting from large and localized deformation. Moreover, the shape of trimmed edge was significantly impacted by ductile fracture which is hard to model[29]. Hubert et al. [30] utilized sequential methodology by extruding 2D trimming model into 3D model which made sure the models inherit information from blanking process. By modified DEFORM-2D method, Taupin et al.[31] simulated the material trimming fracture and able to obtain each zones of trimmed edge. X. H. Hu et al. [10] first predicted crack initiation site as well as the effect on clearance on the burr size for T4 aluminum. The trimming simulation result could be carried into the following stretching or hole expansion simulation and predict the ductility of the sheared surfaces. Besides material simulation, the numerical method was also utilized to simulate tool wear and predict the effect of different process parameters on tool life[32].

In this study, the effect of four trimming parameters (clearance, support condition, upper and lower tool sharpness) and trimmed edge geometery (rollover, burnish, fracture, burr size and roughness) on trimmed edge stretchability is studied. Besides the conventional trimming method, multiple new trimming strategies (low temperature trimming, multiple-stage trimming and trimming by upper tools with various rake angles) are utilized and studied. These strategies are selected based on report from the literature describing the improved edge stretchability or edge quality for different material, yet the effect of these strategies on trimmed edge quality of aluminum material has not been studied. Hence, the mainly objectives in this study are to:

a. Statistically determine a model to predict the material edge stretch and figure out the significant parameters during the trimming process and the optimal trimming condition with maximum edge stretch.
b. Determine a robust range of lower and upper tools radius to get a high edge stretch level.
c. Investigate the influence of multiple trimming strategies, such as low temperature trimming and multiple-stage trimming, on the edge stretchability. Figure out the optimal trimming conditions and strategies.

# Chapter 2: Optimization of the Trimming Parameters

## 2.1 Introduction

The use of existing manufacturing processes are challenged by the significant increase in the utilization of light weight metals, specifically aluminum alloys, in the automotive industry driven by the need to produce fuel-efficient vehicles. A variety of shear cutting technologies are used by the sheet metal industry. Compared to other cutting method, such as laser cutting and water jet, the trimming process is extensively used by the automotive industry driven by speed and cost advantages[3]. The sheared edge quality resulting from the trimming process directly influences the strechability and flangeability of the sheared aluminum sheet in stamping. In this work, the effect of trimming parameters on the edge quality is investigated using experimental and statistical approach.

Investigating sheet metal fracture in trimming is essential for improving robustness and reducing scrap rate in stamping. To understand the induced damage under trimming conditions, the deformation mechanisms controlling the shearing process should inspected. After the tools are in contact with the blank a region of intense shear stress develops, referred to as the plastic zone, and is accompanied with bending caused by the offset loading, that will ultimately lead to failure. The extent of the plastic zone depends on the materials properties and the trimming process parameters[7], [8]. Therefore, the shear edge quality depends on the extent of the plastic zone and hence the trimming process parameters, such as clearance (the distance between upper tool and lower tool), upper and lower tools edge geometry, cutting angle and scrap support etc. The sheared edge geometry has several distinct geometrical features, namely rollover, burnish, fracture, burr and roughness. Studying the evolution of the shear edge geometrical features helps estimate the extent of the plastic zone, the induced damage and

therefore provide an efficient optimization tool of the trimming process. The formation of the shear edge geometrical features is depicted in four distinctive stages: (1) rollover is formed by the plastic deformation of the sheet of metal (under compressive loading) resulting from the contact of the blank with the upper tool. (2) while the upper tool continues its movement downward, a high shear deformation zone is formed resulting in a smooth and flat area named burnish in the sheared edge. (3) As the upper tool continues its movement, two cracks initiate from the edge of the upper and lower tools that propagate and meet forming a rough area named fracture. (4) For some trimming conditions where the material flow significantly, the burr zone is formed. The surface of the fracture area is rough. In this work, fracture roughness is defined as the standard deviation of the cross-section line cut along the sheared edge through the middle of the fracture area.

The clearance is the distance between the upper and lower trim tools. The clearance is usually reported as percentage of materials thickness. Clearance between the trim tools controls the extent of plastic deformation (plastic zone) applied on the material around the trimmed edge. Hence, increasing the clearance induces an increase in the size of the plastic zone and therefore more burr will be observed[9]. X. Hu et al.[10] reported that burr appears in conventional trimming conditions when the clearance is above 20% and consequently contribute to the decrease in edge stretch response. Golovashchenko and Ilinich[22] studied the mechanisms of burr generation and their influence on advanced high strength steel (AHSS) stretchability. The authors reported that higher clearance results into a decrease in the formability in stretch flanging. A design of experiment (DOE) base analysis was used by Hambli[12] to optimize the clearance that minimize blanking force, reduce tool wear and maximize sheared edge quality. Faura et al.[13] used finite element modeling (FEM) coupled with the Crockroft and Latham fracture criterion to optimize the clearance of an AISI 304 sheet. The authors report a good agreement between the experimental and numerical results. Golovashchenko[14], [15] used elasto-plastic FEM model in plane strain formulation to analyze the effect of clearance on the formation of burr. Hu et al.[16] implemented numerical simulations on the trimmed edge stretchability of aluminum and showed that small clearance led to shear type failure and larger elongation, which because samples with smaller clearance

has a more uniform plastic strain distribution that delays localization in the form of shear type failures, leading to higher edge stretch. Moreover large clearance led to splitting type failure and smaller elongation.

The effect of tool radius on edge quality was studied by Li[17]. The author reported that burr height increases with increasing tool radius. Moreover, the authors discussed the influence of tool radius on the blanking force and the effect on the sheared edge geometry. Golovashchenko[21] experimentally investigated the effect of evolving tool radius on the stretching performance and on eliminating slivers. It was suggested to machine a small radius on the upper tool and to limit the clearance to several percent of the material thickness. Wang et al.[8] used a two-step phenomenological Pre-Damage Mapping Mode (PDMM) and a simplified PDMM model for the prediction of the sheared edge of a hole blanked AHSS. It was reported that tool wear increases considerably residual damage in the shear affected zone.

Golovashchenko[19] reported that in conventional trimming conditions cracks initiate and propagate in the aluminum blank from both the upper and lower shearing edges for clearances less than 20%. However, cracks are more developed at the upper shearing edge. Furthermore, for clearances above 20% cracks initiate and propagate only from the upper shearing edge. The author attributed those observations to the bending of the offal that changes the symmetry of the shearing process by adding tensile stresses to the upper edge and compression stresses to the lower edge. Hence Golovashchenko[19] proposed a modification to the conventional trimming process, in which a supporting force on the offal is added to reduce the offal rotation. The authors demonstrated that bending is eliminated by adding mechanical support to the offal, which resulted into reducing burr size and eliminating slivers. Furthermore, Golovashchenko and Ilinich[22] reported that with the clearances between 20%-40%, the modified trimming condition produces smaller burrs than conventional trimming condition. Furthermore, the stretchability of trimmed aluminum sheets in modified trimming condition is reported to be larger than in conventional trimming condition. However, for smaller clearances, the difference between the stretchability of trimmed aluminum sheets with modified and conventional trimming conditions are statistically insignificant. Later, Golovashchenko and Ilinich[22] and Hu[16] investigated the fracture mechanisms and burr reduction in the modified trimming

condition using experimental method and numerical simulations. It is reported that an inherent axisymmetric membrane constraint acts to resist offal rotation, and therefore, reduces the onset of burrs.

Burrs are geometrical imperfections in the sheared edge resulting from the material's plastic flow. Burrs may create difficulties in stamping operations. The burrs are the major source of early fracture when stretching is applied along the sheared edge. Hence, eliminating burr in the blanking process is important for edge quality improvement. Golovashchenko and Ilinich[22] showed that increasing clearance results into an increase of the burr size. Li[17] investigated experimentally the possibility of burrs elimination by combining cutting angle and clearance. The burr height is very sensitive to trimming parameters and a deviation from optimal cutting conditions would result into an increase of the burr height. Golovashchenko[19], [23] used numerical analysis to investigate the mechanisms of burr generation in conventional trimming. The author studied the effect of burr height on the fracture. Le et al.[24] presented an extensive experimental trimming study performed on aluminum alloy to demonstrate the effects of cutting clearance on the sheared edge quality. The authors concluded that the stretchability decreased with increasing burr size. Wang and Golovashchenko[25] investigated the fracture mechanism of sheared aluminum edge. It is reported that when stretching the sheared edge, small cracks initiate at the burr tip and propagate perpendicular to the sheared surface leading to early fracture.

The rollover is the top rounded zone induced by compressing the blank by the upper tool. Suliman[26] experimentally investigated the evolution of the sheared edge geometry with trimming parameters and concluded that the rollover increases with increasing clearance. Hilditch and Hodgson[27] compared the rollover depth of different materials and found that the rollover of steel increase with increasing clearance faster than rollover developed for Al and Mg. The different rollover depth mainly comes from the different ductility and work hardening of those material.

In this study, four trimming parameters are taken into consideration: clearance, support condition, upper and lower tool sharpness. Because these parameters are very common in

production blanking operations, while the explicit effects of these parameters on edge stretchability has not been studied. Hence, the mainly objectives in this study are to:

a. Statistically determine a model to predict the material edge stretch and find an optimal trimming condition with maximum edge stretch.
b. Determine a robust range of lower and upper tools radius to get a high and even edge stretch level.

## 2.2 Experimental material and equipment

### 2.2.1 Materials

The material used in this study is a 6xxx series aluminum sheet of 0.9 mm thickness widely used for stamping outer vehicle body panels. The age hardening of the 6xxx series aluminum alloy results into a variety of microstructural conditions. The dissolution, growth or coarsening of Si- and Mg-rich precipitates results into the age hardening of the materials[33][34]. The microstructural changes induced by the maximum aging temperature and heating rate would have a great influence on the mechanical properties of 6xxx series aluminum. Furthermore, new phase components can be formed in the presence of transition metals such as Fe and Mn. In the casting process, among aluminum dendrites, intermetallic phases such as Al–Fe, Al–Fe–Si and Al–Fe–Mn–Si are formed. β-Fe2Si2Al9 or α-Fe3SiAl12 are the iron rich phases when chromium or manganese are absent. However, α-(Fe, Mn)3SiAl12 or α-(Fe, Cr)3SiAl12 are the formed iron-rich phase in the presence of manganese and chromium induced by the stabilized (Fe, Mn, Cr)3SiAl12[33]. The nominal chemical composition of the studied 6xxx series aluminum alloy is given in Table 2.1. The material was studied in T4 temper after a substantial amount of natural age. All samples used in this investigation are stored at -50ºC to delay age hardening process. Before trimming the samples are left to warm up at room temperature for 1 hour. After trimming the sample are again stored at -50ºC waiting for the mechanical characterization. The samples are again left to warm up at room temperature for 1 hour before conduction the mechanical characterization. The low temperature storing conditions mentioned above are used to ensure that all the processed and characterized material are within the same hardening window and therefore the results variability induced by age hardening difference is eliminated or reduced.

Table 2.1: Chemical composition and corresponding weight percent

| Element | Si | Mg | Fe | Cu | Mn | Cr | Zn | Ti | other |
|---|---|---|---|---|---|---|---|---|---|
| Wt% | 0.5-1 | 0.4-0.8 | 0.3 | 0.2 | 0.15 | 0.1 | 0.1 | 0.1 | 0.15 |

### 2.2.2 Specimen design

The specimen geometry used in this study is presented in figure 2.1. This type of geometry is referred to as half dog bone (HDB) and is frequently used in sheared edge research. The geometry of the specimen is designed to meet two basic requirements: a) improve the trim line alignment and parallelism to the opposite edge during trimming, b) localize the deformation in the center region of the specimen away from tensile frame grips during tensile testing. The first requirement is addressed by the presence of a reduced width gage section. The second requirement is addressed by the presence of the alignment slots in the specimen and the corresponding locating pins on the lower tool. The specimens were wire electro discharge machined (wire EDM) from aluminum sheet to reduce the influence of the machined edges on the sheared edge performance.

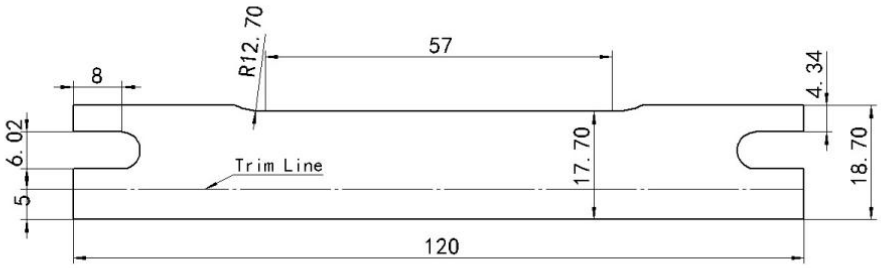


Figure 2.1: Geometry of the specimen, dimensions in mm

### 2.2.3 Experiment procedure and equipment

In this section, the experiment equipment and procedures used in this study are presented.

2.2.3.1 Trimming process

The half dog bone specimens presented earlier are trimmed to remove along the trim line a strip of approximately 5mm in width. An illustration of the trimming process is presented in figure 2.2(a). The blank is clamped between the lower tool and the pad with almost constant clamping force. When the upper tool is in contact with the blank, a localized plastic area between the blade edges of the upper and the lower tool is formed that results into fracture. The

trimming experiments are performed on a phi Pasadena hydraulics, trimming machine that is shown in Figure 2.2(b).

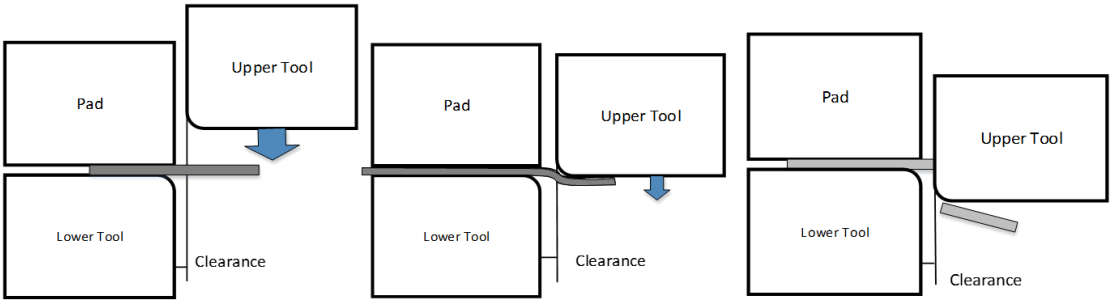


(a)

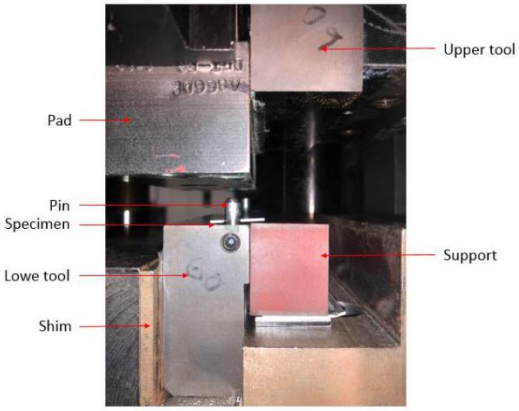


(b)

Figure 2.2: (a) Schematic representation of the trimming process (b) Trimming machine side view.

In this study, five trimming parameters are varied in the purpose of optimizing the trimmed edge quality, namely; the clearance, the upper tool blade radius, lower tool blade radius and presence of support. The support is a polymer block aligned with the lower tool upper surface used to resist the offal rotation. The sheet trimming direction represents the sheet direction relative to the rolling direction along which the trimming process in conducted. In this study, the trimming is conducted only along the transverse to the rolling direction (TD). The upper tool and lower tool blade radius represent the sharpness of the tools cutting edges. The upper and lower tools are micro-machined using a 1 μm diamond tool. A 3D optical microscope is utilized to measure the upper and lower tools radius. The actual and design tool radius and standard deviation of every tool measurements are shown in table 2.2. The difference between

the design and actual radius values are within acceptable range which clearly highlight the capability of the micro-machining method to manufacture controlled edge sharpness. In this work, the actual tool radius is used to differentiate between the different tool geometries.

Table 2.2: The actual and design tool radius and standard deviationμ

| | **Intended (μm)** | **Measured (μm)** | **Standard deviation of the measured (μm)** |
|---|---|---|---|
| Lower sharp | 0 | 2 | 0.1826 |
| Lower 10R | 10 | 16 | 2.1992 |
| Lower 30R | 30 | 40 | 1.8166 |
| Lower 50R | 50 | 54 | 2.3764 |
| Lower 100R | 100 | 103 | 2.9790 |
| Upper sharp | 0 | 2 | 1.6025 |
| Upper 30R | 30 | 30 | 1.5297 |
| Upper 100R | 100 | 102 | 1.7174 |

Table 2.3 details the experimental matrix. Six repetitions for every combination of parameters is performed, five specimens are used for tensile characterization and one for microstructural analysis. In this study, two values of the clearance are chosen, 10% and 30%. Those values are the most relevant for industrial applications. In this study, the trimming operation are either performed with no support or with high support in which offal rotation is not allowed. In figure 2.2(b) shows that the lower tool was fabricated in a die shoe providing sufficient tooling alignment for uniform clearance during installation and maintaining consistent clearance with stiff guiding strategies to prevent increase of clearance during operation. The upper tool is fixed with small tolerances on the trimming machine, to keep a constant position during the trimming operation. The clearance in our experiments are achieved by inserting an appropriate combination of shims between lower tool and shoe die. The clearance is verified by inserting a combination of precision gauge block and gage shims between the lower and the upper dies. Figure 2.2(b) shows a locating pin on the top surface of the lower tool (another pin is located at the opposite side) that is designed to position the half dog-bone specimen.

Table 2.3: Parameters varied during experimental investigation.

| **Parameters** | **Level** |
|---|---|

| | |
|---|---|
| Upper tool shape | 2µm, 30µm, 102µm |
| Lower tool shape | 2µm, 16µm, 40µm, 54µm, 103µm |
| Clearance | 10%, 30% |
| Support | No support, High support |
| Direction | TD |
| Repetition | 5+1 |
| total | 360 |

2.2.3.2 Edge geometry measurements via 3D optical microscopy

A Digital 3D Microscope (VHX-5000 Series by Keyence) is used to analyze the edge geometry and measure its features (rollover, burnish, fracture, burr and roughness). Compared to conventional optical microscopes, the 3D Microscope captures the out-of-plane geometry of the viewed object. Several images are captured automatically by adjusting the focal distance. The images are then stitched along the out-of-plane direction to obtain an infinite focal depth image and reconstruct the 3D profile of the object. Four 3D microscope parameters are tuned in this work to ensure a clear 3D profile, namely; the lower and upper scanning bound, images stitching setting and magnification. The specimens are clamped with the shared edge facing the lens. A MATLAB code is used to analyze the 3D profile of each sample to determine the size of the rollover, burnish, and fracture areas, and also to measure the burr and fracture roughness.

As example, the 3D profile of a sheared edge is shown in figure 2.3(a). Figure 2.3(b) shows one cross section line that is extracted to measure the four edge geometry features (rollover, burnish, fracture and burr). The rollover is set to start at point A (selected when the slope of the curved presents finite values), the end of the rollover and start of the burnish point B is selected when the slope of the curve tends to zero. Point C, end of burnish and start of the fracture zone is determined by selecting the last point that present the same height as point B. The point D, considered as the end of the burr zone, is determined by selecting the point that present a significant decrease of the slope. Finally, a line along the longitudinal direction of the specimen

in the middle of the fracture zone is extracted and the roughness is computed as its standard deviation.

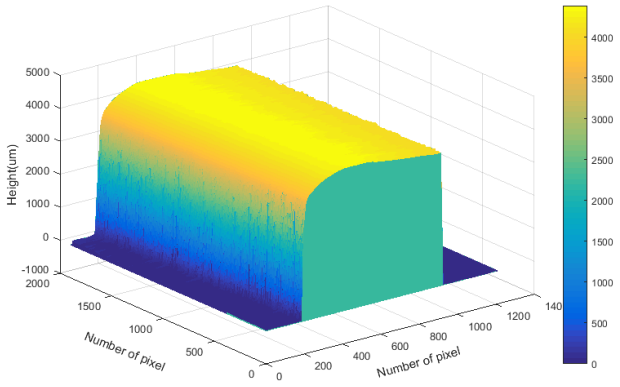


(a)

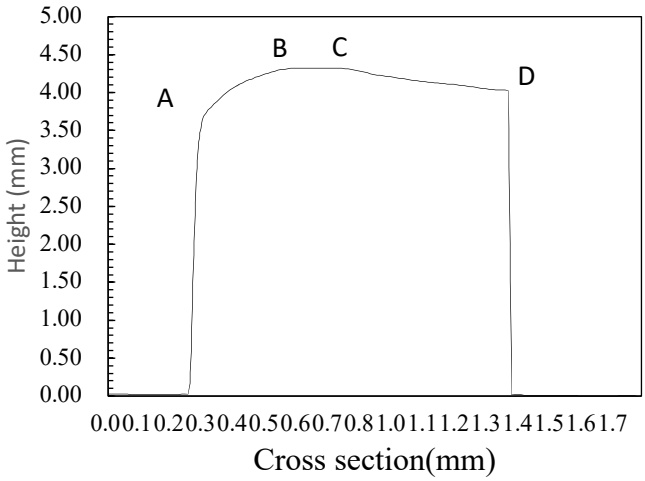


(b)

Figure 2.3: (a) 3D edge profile scanned by microscope, (b) Cross section profile of a trimmed edge

2.2.3.3 Edge stretchability evaluation

Edge stretchability is evaluated by tensile testing with global and local strain measurements. The tensile test experiments are performed at room temperature with the help of a universal electromechanical testing machine, Instron 4469, equipped with a 50 kN load cell. The full-field measurement of displacement and strain are achieved using an ARAMIS 3D Digital Image Correlation (DIC). Prior to testing the specimens, an evenly distributed speckle pattern is deposited on white painted surface. To avoid paint peeling and capture the field deformation

until complete fracture, the specimens are tested within 4 hours after painting. The specimens are tested at a constant cross-sectional speed of 4mm/min. In DIC system, the facet size and point distance are 20 pixels and 14 pixels respectively. The DIC system is set to capture 4Hz and the buffer with 20Hz and 8 second length is introduced to capture more stages prior to fracture and increase the results accuracy. During DIC post-processing, the global strain is measured along a 2in gage line centered along the physical gage length of the specimen. As general observation, two type of fractures are observed, namely; fracture through crack initiating at the edge or in the center of the specimen. When the fracture is induced by cracks initiating at the edge of the specimen, the crack propagation is gradual. While, a more abrupt fracture is observed when the cracks initiate at the center of the specimen. Therefore, the local strain is defined as the maximum major stain before the crack initiation for specimen with crack initiating at their center, and as major stain at crack initiation point before the crack initiation for specimen with crack initiating at their edge. The mechanical properties of the wire EDM specimen (not trimmed) are used to understand properties degradation induced by the trimming process. The average total elongation to fracture of five wire EDM specimens (not trimmed) is 25.82%

2.2.3.4 Metallography

The specimens were prepared for microstructural investigations according to the following procedure. First, 12.70x10x0.9mm specimens cut along the cross-section were mounted in a phenolic resin powder using a hydraulic-pneumatic automatic mounting press. The specimen is mounted to allow observing the microstructure in the cross-sectional area of the half-dog bone specimens. Then mounted samples are grinded with sandpaper in the consecutive order of grades 240 grit, 400 grit, 600 grit, 1200 grit and 2400 grit. Between each step, the specimens are rotated by 90° and washed with alcohol and water used as lubricant. Polishing was implemented using abrasive slurries in the consecutive order of grades 5μm, 3μm, 1μm and 0.3μm until the clear, haze-free mirror surface is achieved. To prevent polishing compound from embedding into the aluminum matrix the specimens were gently pressed against the grinding and polishing disks. After polishing, the samples were etched by automatic etching machine Electromet 4 for 2 minutes. The bath composition used in Electromet 4 consist of

orthophosphoric acid, amyl alcohol and distilled water. The specimens were immersed in the etchant solution for two minutes then rinsed with alcohol. The microstructure is observed using a Olympus BX51optical light microscope equipped with an ERc5s camera connected to a computer.

## 2.3 Results

In this section, the trimmed edge and tensile properties evolution with the different combination of trimming process parameters are presented.

### 2.3.1 Trimmed edge geometry

Geometrical properties of the trimmed edge, namely; rollover, burnish, fracture, burr and fracture roughness are measured and presented as boxplot for different combinations of trimming process parameters.

The figure 2.4 presents the effect of different process parameter on the distribution of the rollover size. Figure 2.4(a) shows the effect of the clearance change on the rollover size. When the clearance is increased from 10% to 30%, the rollover size and the standard deviation increase significantly. Indeed, for 10% clearance the data points are close to the mean value while in comparison a more spread out data can be noticed for 30% clearance. Furthermore, the distribution changes from symmetric for 10% clearance to right-skewed for 30% clearance. Figure 2.4(b) presents the effect of upper tool radius on the rollover size. It is observed that the rollover size slightly increases with the upper tool radius increase, but there is no noticeable change of the standard deviation. The effect of the lower tool radius on the rollover size is presented in figure 2.4(c). No clear trend is observed for the rollover size evolution with increasing lower tool radius. Finally, figure 2.4(d) presents the effect of the presence of a support on the rollover size. It is observed that using an offal support slightly increases the mean value of the rollover size with a clear increase of the standard deviation. Furthermore, the distribution changes from symmetric for conventional trimming to right-skewed for offal supported trimming.

(a) (b)

(c) (d)

Figure 2.4: Boxplots of the Rollover size distribution with variable trimming process parameters.

The figure 2.5 presents the effect of different process parameter on the distribution of the burnish size. Figure 2.5(a) shows that the burnish size and the standard deviation decrease with increasing clearance from 10% to 30%. Furthermore, the data distribution changes from right-skewed for 10% clearance to left-skewed for 30% clearance. Figure 2.5(b) shows a decrease of the average burnish size and the standard deviation with increasing the upper tool radius. Figure 2.5(c) shows that with increasing the lower tool radius the mean value of the burnish size increases until radius reaches 40 μm and remains stable afterwards. The figure does not show any noticeable change of the standard deviation. Finally, figure 2.5(d) shows that the conducting trimming while using an offal support decreased both the mean value of the burnish size and its standard deviation. Furthermore, the distribution changes from right-skewed for no offal support trimming to symmetric for offal support trimming.

(a) (b)

(c) (d)

Figure 2.5:Boxplots of the Burnish size distribution with variable trimming process parameters.

The figure 2.6 presents the effect of different process parameter on the distribution of the fracture size. As a general observation, the evolution of the fracture size distributions as function of the different process parameters follows an opposite trend to the one observed for the burnish. Similar observations are reported in the literature by Wu and Bahmanpour[35] who reported that the total size of both the burnish and fracture stays constant. Figure 2.6(a) shows that the fracture size increased while the standard deviation decreases with increasing clearance from 10% to 30%. Furthermore, the data distribution is left-skewed for both clearance values. Figure 2.6(b) shows an increasing trend of the mean fracture size and no clear trend of the standard deviation with respect to the upper tool radius. The effect of the lower tool radius on the fracture size presented in figure 2.6(c) shows no clear trend. Finally, figure 2.6(d) shows that the conducting trimming while using an offal support increases the mean value of the fracture size with a clear decrease of the standard deviation.

(a) (b)

(c) (d)

Figure 2.6: Boxplots of the Fracture zone size distribution with variable trimming process parameters.

The figure 2.7 presents the effect of different process parameter on the distribution of the burr size. Figure 2.7(a) shows that the burr size and the standard deviation increased with increasing clearance from 10% to 30%. Furthermore, the data distribution is right-skewed for both clearance values. Figure 2.7(b) shows an increase of the mean burr size and standard deviation with increasing upper tool radius. The effect of the lower tool radius on the burr size presented in figure 2.7(c) shows an increase of both the mean burr size values and standard deviation. Finally, figure 2.7(d) shows that offal support utilization decreases the mean value of the burr size and its standard deviation.

(a) (b)

(c) (d)

Figure 2.7: Boxplots of the Burr size distribution with variable trimming process parameters.

The figure 2.8 presents the effect of different process parameter on the distribution of the fracture roughness. Figure 2.8(a) shows that the mean roughness value slightly increase and the standard deviation slightly decrease with increasing clearance from 10% to 30%. Additionally, the data distribution is right-skewed for both clearance values. Figure 2.8(b) shows an increase of the mean roughness with increasing upper tool radius. No noticeable change of the standard deviation is observed. The effect of the lower tool radius on the roughness, presented in figure 2.8(c), shows no clear trend in the evolution of the mean roughness values and standard deviation. Figure 2.8(c) shows only a slight increase of the roughness and the standard deviation for tool radius smaller than 16 µm. Finally, figure 2.8(d) shows that the conducting trimming while using an offal support decreases the mean value of the roughness while keeping a constant standard deviation.

(a) (b)

(c) (d)

Figure 2.8: Boxplots of the Roughness distribution with variable trimming process parameters.

### 2.3.2 Trimmed edge ability to stretch

In this section, the measured edge stretch of trimmed specimens at different process parameters is compared using both global and local elongation metrics. More precisely, the distribution of the total elongation and the local stain at fracture in tensile tested specimens obtained with variable trimming process parameters are presented in boxplots and scatterplots. Furthermore, the fracture initiation location captured by DIC is analyzed and a correlated with the different trimming conditions. Finally, the load-displacement curves for specimens exhibiting different fracture initiation locations are studied.

The total elongation in this section refers to the total engineering strain at failure, computed by following using the DIC system the deformation of a 2” digital gage. Therefore, the ratio between the change in length of the digital gauge at the onset of fracture and the original length is considered as the total elongation. The total elongation of the wire EDM specimen is included as the baseline for comparison and is highlighted in red lines in the boxplots.

The figure 2.9 presents the effect of different process parameter on the distribution of the total elongation. Figure 2.9(a) shows the effect of the clearance change on the total elongation. When the clearance is increased from 10% to 30%, the total elongation decreases while the standard deviation increase. The mean of wire EDM specimen total elongation is comparatively close to the total elongation mean value of the 10% clearance specimens. Figure 2.9(b) presents the effect of upper tool radius on the total elongation. It is observed that the total elongation decreases significantly with increasing upper tool radius, accompanied with an increase of the standard deviation. This observation clearly demonstrate that the sheared edge stretch is sensitive to the dullness of the tool. The effect of the lower tool radius on the total elongation is presented in figure 2.9(c). although the trend is not strong, some decrease of the total elongation with increasing lower tool radius is observed. The total elongation is less sensitive to the lower tool radius variation. Therefore, in the industrial environment, the lower tool may have longer life cycle than the upper tool. Finally, figure 2.9(d) presents the effect of the presence of a support on the total elongation. It is observed that the conducting trimming while using an offal support increase the mean value of the total elongation with some decrease of the standard deviation. Furthermore, the distribution changes from right-skewed for no offal support trimming to symmetric for offal support trimming

(a) (b)

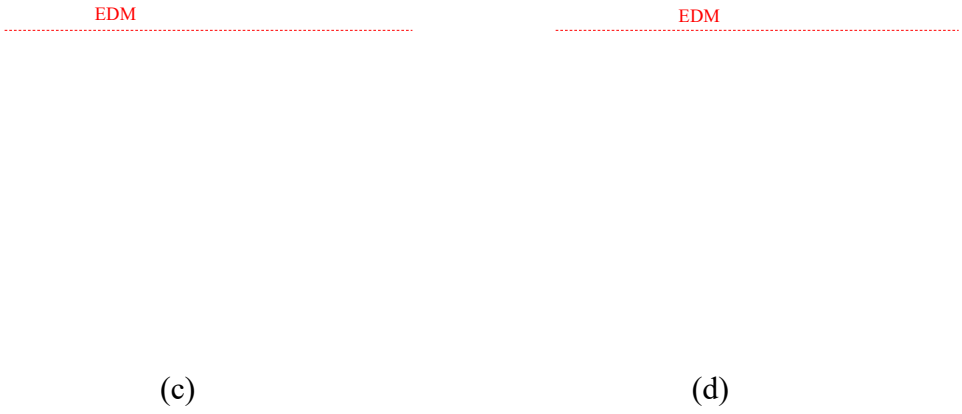


(c) (d)

Figure 2.9: Boxplots of the Total elongation distribution with variable trimming process parameters.

To better understand the effect of the offal support on the total elongation of tensile test specimens, the results are presented as scatter plots. Figure 2.10 presents the total elongation of specimen trimmed at different process parameters (with five repetitions) are presented separately for high support and no support conditions. It can be noticed that specimens trimmed with sharp upper tool (R=2 µm) and high support exhibit lower average total elongation than specimens trimmed with the same condition but with no support. However, the conclusion proposed based on the results of figure 2.9(d) holds true for samples trimmed with upper tool radius higher than 2 µm. It can be argued that using high support reduces the contact force between the blank and the lower tool edge while eliminating bending. As known, the edge sharpness promotes stress localization resulting into a narrower plastic zone and hence better edge properties. We can assume the existence of two mechanisms acting in opposite directions; first, decreasing the extent of the plastic zone with increasing upper and lower tools edge sharpness and second, increasing the extent of the plastic zone with decreasing contact force between the blank and the lower tool. Therefore, the presence of support when trimming with high sharpness upper tool decreases the extent of the plastic zone (resulting from the contact between the blank and lower tool edge) but less than if there is no support. Hence, for this particular trimming condition the presence of support is not beneficial. Furthermore, Figure 2.10, shows that the total elongation is insensitive to the presence of offal support for specimens trimmed with the sharpest lower tool (2R). The total elongation is improved considerably when using offal support for specimens trimmed with dull upper tool. Finally, the average total

elongation is improved when using offal support for specimens trimmed with a clearance of 30%.

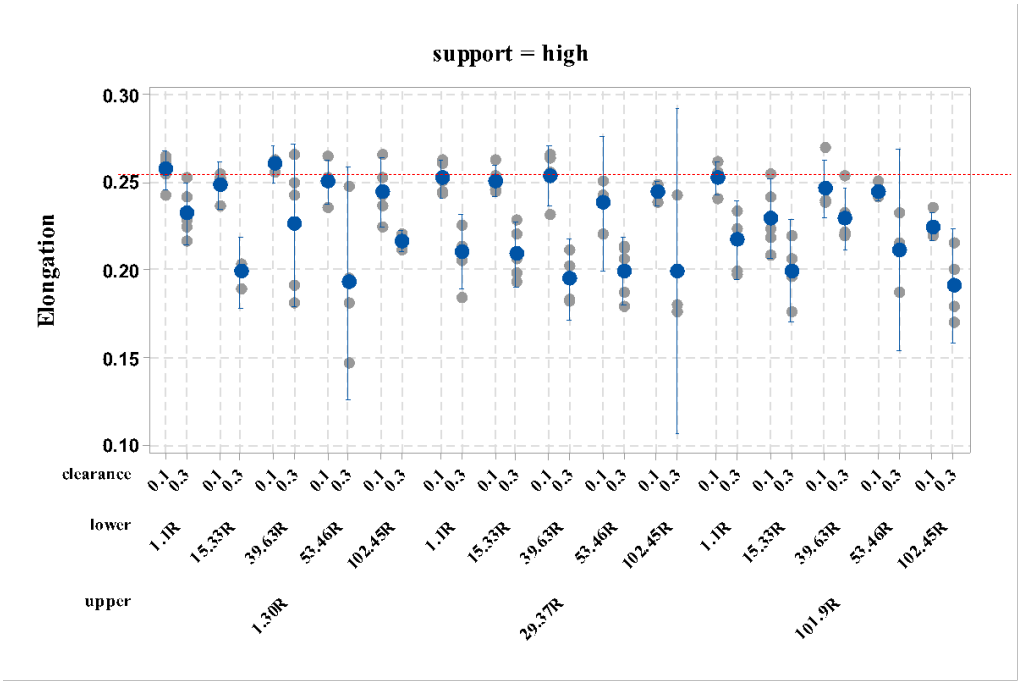


(a)

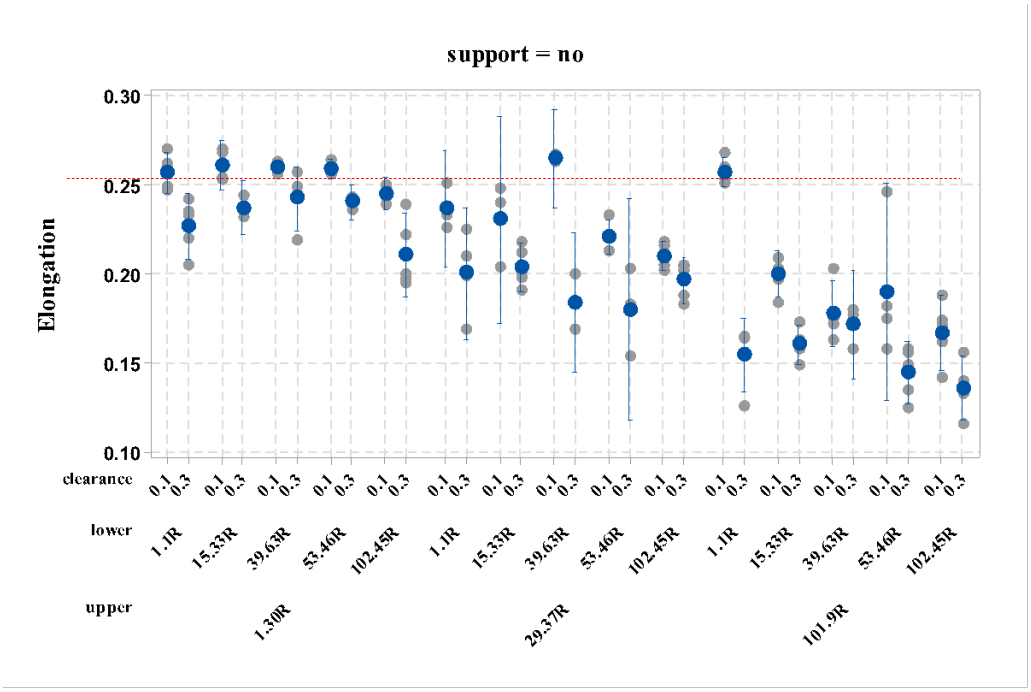


(b)

Figure 2.10: Scatter plot of the Total elongation distribution with variable trimming process parameters, (a) with support (b) without support.

Section 2.4.3 detailed the procedure used to extract the maximum local strain during tensile testing. In summary, the maximum local strain is the maximum major strain at fracture. The fracture is assumed to be the crack initiation for specimen with crack initiating at their center, while it is assumed to be the complete fracture for specimen with crack initiating at their edge. The figure 2.11 presents the effect of different process parameter on the distribution of the maximum local strain. Figure 2.11(a) shows the effect of the clearance change on the maximum local strain. When the clearance is increased from 10% to 30%, the maximum local strain decreases while maintaining a symmetric distribution and a constant standard deviation. Figure 2.11(b) presents the effect of upper tool radius on the maximum local strain. It is observed that the maximum local strain decreases with the upper tool radius increase with noticeable change of the standard deviation. The effect of the lower tool radius on the maximum local strain is presented in figure 2.11(c). A decrease of the maximum local strain with increasing lower tool radius is observed. Finally, from figure 2.11(d), it is observed that conducting trimming while using an offal support has no effect on the mean value of the maximum local strain although a slightly decreased standard deviation is noticed. Similar trends are noticed in the distribution evolution of the maximum local strain and the total elongation with different process parameters except for the effect of the support.

(a) (b)

(c) (d)

Figure 2. 11: Boxplots of the maximum local strains distribution with variable trimming process parameters.

The DIC system allows capturing images at higher frequency just before complete failure of the tested specimen. Therefore, the location of fracture initiation either in the center or at edge of the specimen can be determined accurately as shown in figure 2.12(a) and figure 2.12(b). As mentioned previously, specimens with crack initiating at the center exhibit very high deformation post initiation. While specimens with crack initiating at the edge exhibit lower post initiation deformation. Moreover, only specimens with crack initiating at the center exhibit localized necking. A fracture surface perpendicular to the loading direction is observed for the specimens with edge cracks initiation while the specimens with center cracks initiation presents a shear type fracture surface. Similar observations are reported by Le and Golovashchenko[24] who identified three failure mechanisms associated with trimmed edge. When comparing the load vs displacement curves of specimens trimmed with the same process parameters however exhibiting different crack initiation modes, the specimens with edge cracks presents lower stiffness and ductility (figure 2.12(c)). Specimens with edge crack initiation presents lower trimmed edge surface quality than those with center crack initiation[14].

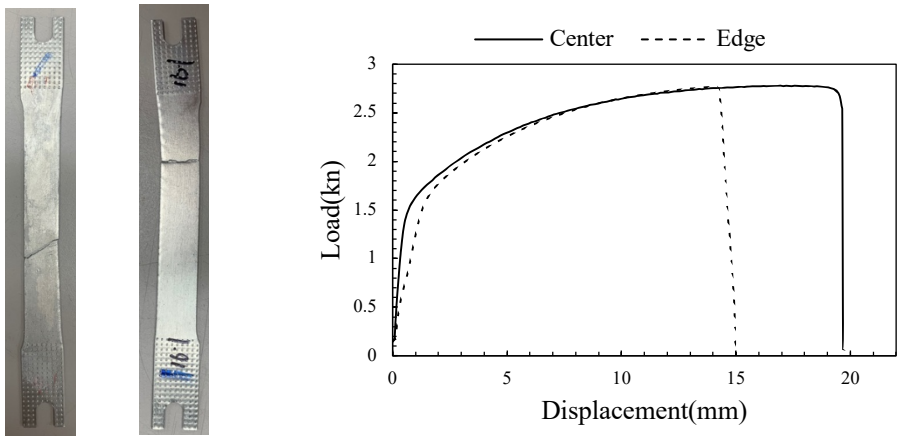


(a) (b) (c)

Figure 2.12: (a) Crack initiating at the center (b) Crack initiating at the edge (c) Load-displacement curves exhibited by specimen fracturing at three different fracture modes.

The percentage of specimens presenting center crack initiation is documented for different trimming condition and the results are presented in figure 2.13. The results present high correlation with the one presented in Figures 2.9 and 2.11. Figure 2.13(a) shows that the percentage of specimens with center crack initiation decreases significantly when increasing the clearance from 10% to 30%. A significant decrease in the percentage of specimens presenting center crack initiation is noticed when increasing the upper tool radius (Figure 2.13(b)). A more gradual decrease of the percentage of specimens presenting center crack initiation is observed when increasing the lower tool radius (Figure 2.13(c)). Finally, figure 2.13(d) presents almost no difference in the percentage of specimens presenting center crack initiation when high support or no support is used.

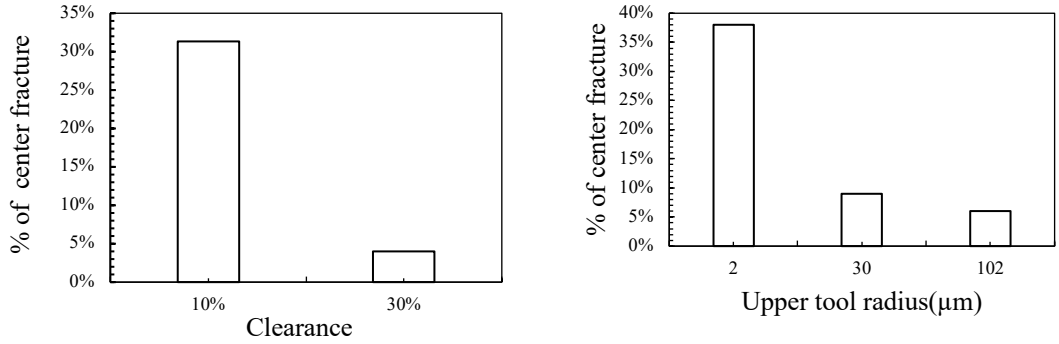


(a) (b)

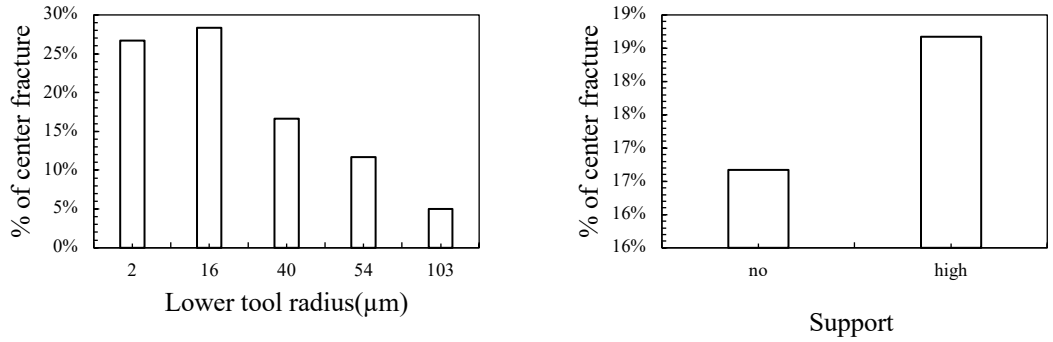


(c) (d)

Figure 2.13: The percentage of center fractured specimens with variable trimming process parameters.

### 2.3.3 Microstructural observation and analysis

The microstructures of the specimen-trimmed edges are observed along the Rolling Direction (RD) and the Normal to the rolling Direction (through thickness) (ND) plane. Figure 2.14 presents the microstructure of the trimmed edge resulting from different trimming process parameters. In total 60 different trimming conditions are analyzed. This figure provides a clear visual of the surface quality. The rollover and the burr size are clear indication of the plastic zone extent during trimming and therefore the damage induced to the trimmed edge surface. We can observe that for high sharpness upper tool edge and no support that the size of both the rollover and the burr are the smallest among all the trimming conditions. Furthermore, the specimens trimmed under those conditions presented the highest total elongation (figure 2.10). Additionally, we can observe that for the dullest upper tool, clearance of 30% and no support that the size of both the rollover and the burr are the largest among all the trimming conditions. Also, the specimens trimmed under those conditions presented the lowest total elongation (figure 2.10). Therefore, it exists a strong correlation between the rollover and burr size and the damage induced to the trimmed edge during processing. Estimating the trimmed edge induced damage can be very useful for optimizing the trimming process parameters.

| | | | | | | | |
|---|---|---|---|---|---|---|---|
| 2R (lower) | No | 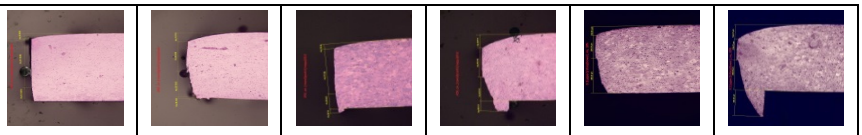 | | | | | |
| | High | 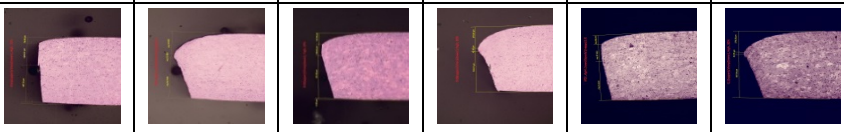 | | | | | |
| 16R (lower) | No | 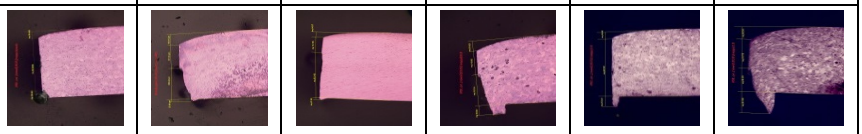 | | | | | |
| | High | 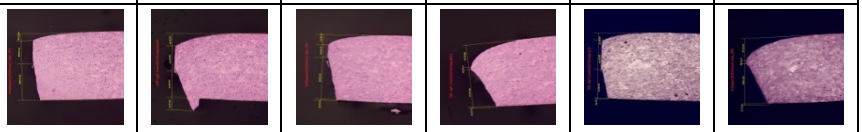 | | | | | |
| 40R (lower) | No | 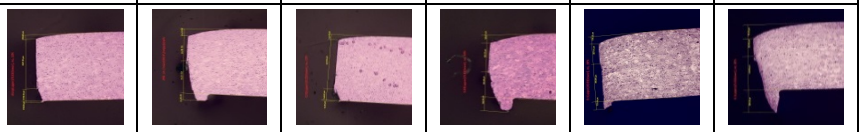 | | | | | |
| | High | 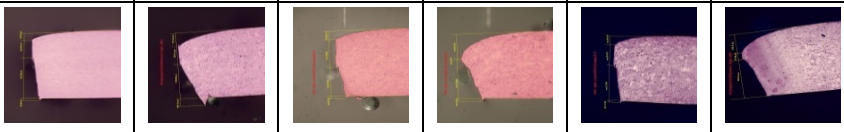 | | | | | |
| 54R (lower) | No | 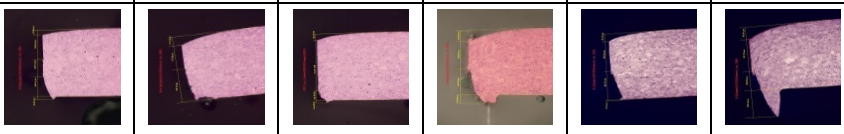 | | | | | |
| | High | 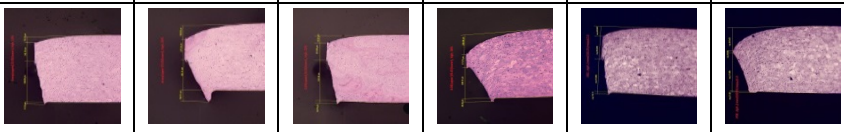 | | | | | |
| 103R (lower) | No | 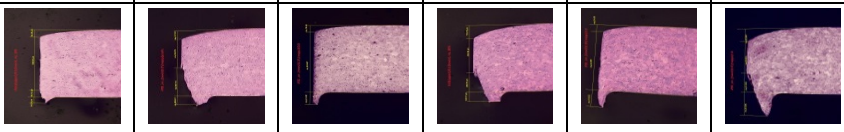 | | | | | |
| | High | 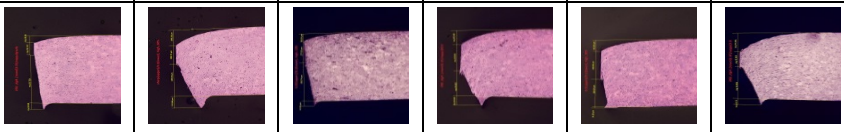 | | | | | |
| | | 10% | 30% | 10% | 30% | 10% | 30% |
| | | 2R(upper) | | 30R(upper) | | 102R(upper) | |

Figure 2.14: Trimmed edge microstructure for different trimming process parameters.

## 2.4 Data Analysis

### 2.4.1 Multivariate linear regression analysis

The results presented in section 3 show the effect of trimming process parameters and the interaction between them on the trimmed edge quality and the edge stretchability. In this section, the Multiple Linear Model regression is used to further investigate the relationship between the edge stretch, edge geometry, and trimming process parameters, and also for identifying the significant processing and edge geometry parameters and their interaction. As a first approach, the interactions between controllable factors (e.g. trimming condition: clearance, support, upper and lower tool radius) are considered. As a second approach the interaction between edge geometry parameters (rollover, burnish, fracture, burr and roughness) are considered. Finally, the third approach a regressing considering the interaction between controllable factors and edge geometry parameters is studied.

The stepwise variable selection method combining the forward and backward passes is utilized for selecting factors and interactions with the most predictive power. Table 2.4, table 2.5 and table 2.6 summarize the explanatory variables, the variables considered for each regression step and for each step the coefficient of determination for the multivariate regression, $R^2$. The $R^2$ ranging from 0% to 100% represents the proportion of the variance in the dependent variable (total elongation) predicted from independent variable (controllable factors and edge geometry parameters). The $R^2$ is a statistical measure used to estimate how close is the regression model from the dataset, hence, with closer $R^2$ to 100% the better is the predictive capability of the regression model.

By selecting the trimming process parameters as explanatory variables and not allowing interaction in the regression equation in table 2.4, it is found that the largest $R^2$ is 57.18%. This $R^2$ value is low and hence the corresponding regression model does not predict the dataset accurately. If the regression equation includes the trimming process parameters as explanatory variables, interaction and second order terms, the last calculation step results into a regression model with an acceptable $R^2$ equal to 71.94%. The resulting regression model representing the total elongation as function of most significant parameters is written as function of four main parameters, four interactions and one second order parameter.

Table 2.4: The predictors and corresponding results of regression analysis by trimming condition

| **Considered explanatory variables** | **step 1 Considered variables** | **$R^2$ in %** | **step 2 Considered variables** | **$R^2$ in %** | **Last step Considered variables** | **$R^2$ in %** |
|---|---|---|---|---|---|---|
| Trimming condition (clearance, support, upper tool, lower tool) **without** interactions and second order terms | clearance | 26.53 | Clearance<br>upper | 45.68 | Clearance<br>upper<br>Support<br>lower | 57.18 |
| Trimming condition (clearance, support, upper tool, lower tool) **with** interactions and second order terms | Upper Clearance<br>Upper*clearance | 45.63 | Upper Clearance<br>Upper*clearance<br>support | 64.84 | upper<br>clearance<br>support<br>upper*support<br>lower<br>upper*lower<br>upper*upper<br>lower*support<br>lower*clearance | 71.94 |

When using trimmed edge geometry parameters instead of the trimming process parameters as explanatory variables in table 2.5, a regression model using only the burr size as variable (after the first step of stepwise selection) results in an $R^2$ equal to 63.46%. As mentioned previously, the burr is the result of the material plastic flow and its size depends on the extent of the trimming process induced plastic zone. According to the first calculation step, the burr size has the most significant correlation with edge stretchability. This result is in accordance to the previously reported observation. From figure 2.14 we can compare two trimming conditions resulting in two different burr size; (a) Lower tool 2R-Upper tool 102R-No support-10% clearance (b) Lower tool 2R-Upper tool 102R-No support-30% clearance. Trimming condition (b) results into the largest burr size. Under tensile loading the trimming condition (b) results into the lowest total elongation before fracture. In second calculation step with both the burr and rollover size are used as regression variables. The regression model presents a significant increase of the $R^2$ values 63.46% to 77.76%. In figure 2.14 the following trimming

condition (c) Lower tool 54R-Upper tool 2R- support-30% clearance results into a very small burr size similar to (a) however larger rollover size. Under tensile loading the trimming condition (c) results into a smaller total elongation before fracture than condition (a). Although a strong correlation between the burr size and the total elongation to fracture, burr size alone cannot correlate with all trimming process conditions. It is clear that the regression model using the trimmed edge geometry parameters as explanatory variables presents better prediction than the one using the trimming process parameters as explanatory variables, which is quantitatively measured by the lower number of significant variables and higher values of $R^2$. The regression model using the trimmed edge geometry parameters as explanatory variables does not present much better correlation in the last calculation step.

Table 2. 5: The predictors and corresponding results of regression analysis by surface geometry parameters

| **Considered explanatory variables** | **step 1 Considered variables** | **$R^2$ in %** | **step 2 Considered variables** | **$R^2$ in %** | **Last step Considered variables** | **$R^2$ in %** |
|---|---|---|---|---|---|---|
| surface geometry parameters (rollover, burnish, fracture, burr and roughness) **without** interactions and second order terms | Burr | 63.46 | Burr<br>Rollover | 77.76 | Burr<br>Rollover<br>fracture | 78.94 |
| surface geometry parameters (rollover, burnish, fracture, burr and roughness) **with** interactions and second order terms | Rollover<br>Burr<br>Burr*rollover | 79.41 | Rollover<br>Burr<br>Burr*rollover<br>Fracture<br>Rollover*fracture | 80.20 | Rollover<br>Burr<br>Burr*rollover<br>Fracture<br>Rollover*fracture<br>Roughness<br>Rollover*roughness | 80.40 |

When the trimmed edge geometry and trimming process parameters are used as explanatory variables in table 2.6, the clearance and the upper tool radius are two most significant variables among the trimming process parameters, while the burr size, rollover size and burnish size are

the most significant variables among the trimmed edge geometry parameters. Finally, in the last calculation step, the resulting regression model representing the total elongation as function of most significant parameters is written as function of seven main parameters, five interactions and one second order parameter. The corresponding $R^2$ is equal to 82.9%, which is the maximum $R^2$ value found among all investigated regression models.

Table 2.6: The predictors and corresponding results of regression analysis by trimming conditions and surface geometry parameters

| **Considered explanatory variables** | **step 1 Considered variables** | **$R^2$ in %** | **step 2 Considered variables** | **$R^2$ in %** | **Last step Considered variables** | **$R^2$ in %** |
|---|---|---|---|---|---|---|
| Trimming condition and surface geometry parameters **without** interactions and second order terms | burr | 63.46 | Burr<br>rollover | 77.76 | Burr<br>rollover<br>Fracture<br>Upper<br>clearance | 79.28 |
| Trimming condition and surface geometry parameters **with** interactions and second order terms | Rollover<br>Burr<br>Burr*rollover | 79.41 | Rollover<br>Burr<br>Burr*rollover<br>Burnish<br>Upper<br>Burnish *upper | 80.63 | burr<br>rollover<br>burr*rollover<br>burnish<br>upper<br>burnish*upper<br>clearance<br>roughness<br>rollover*clearance<br>upper*upper<br>lower<br>lower*roughness<br>clearance*roughness | 82.9 |

### 2.4.2 Main effect and interactions

From the regression result, the burr size is the most significant factor to predict edge stretchability. In this section, the effect of support condition on the correlation between burr size and elongation is discussed. Because in practical, the high support condition which has

significant negative impact on correlation is seldomly utilized as it results into design and install complexity. The correlation between burr size and elongation for no support presents stronger relationship than the correlation between burr size and elongation for high support. For no support, as shown in figure 2.15(b), the data set distributed evenly along the regression line with small standard deviation indicating a relatively high correlation ($R^2$=75.27%). As shown in figure 2.15(c) the use of high support leading to smaller burr size area with relatively high standard deviation decreases the correlation between burr size and total elongation ($R^2$=52.4%).

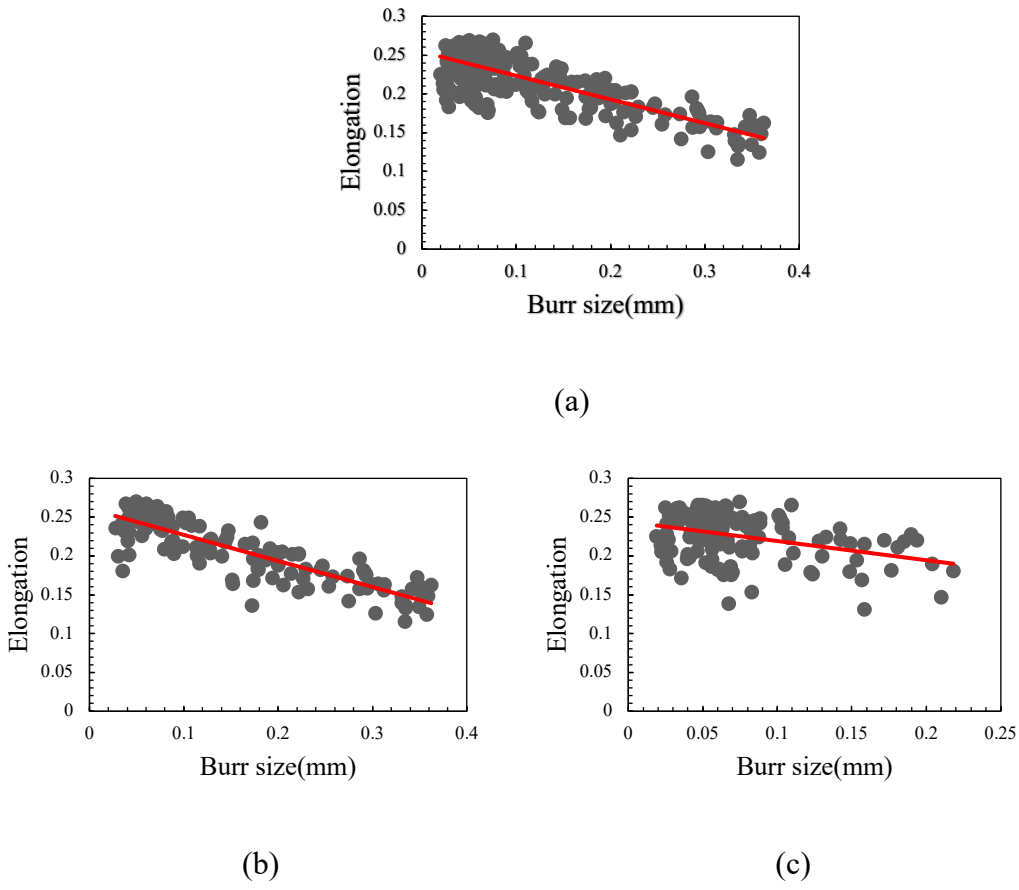


Figure 2.15: (a) Burr size verse elongation (b) Burr size verse elongation with no support (c) Burr size verse elongation with high support

The interaction effects of trimming process parameters on total elongation with different support conditions is shown in figure 2.16. Three interations, upper&lower, upper&clearance and lower&clearance, are consided and shown in each subplot.

For the high support condition, figure 2.16(a), the effect of lower tool radius and upper tool radius on elongation is nonlinear. For upper tool radius ranging between 0 and 0.03mm, evolving the lower tool sharpness has no effect on the elongation. With increasing upper tool radius, the sensitive of lower tool on elongation increases at first and then decreases. The slope of the line in clearance&upper subplot is nearly horizontal which means that the elongation is sensitive to the clearance and less sensitive to the upper tool radius. Because when the upper tool radius is fixed, the elongation changes with clearance significantly. While when the clearance is fixed, the elongation changes slightly with the upper tool radius change. Similar conclusion can also be stated for the clearance&lower subplot, precisely, the elongation is sensitive to the clearance and less sensitive to the lower tool radius.

When it comes to no support condition, figure 2.16(b), the three interactions relationship are all linear. From the lower&upper subplot, the elongation is slightly more sensitive to upper tool radius than lower tool radius, since the slope of the line is slightly higher than 45°. Moreover, from the clearance&upper and clearance&lower tool plot, the elongation is more sensitive to clearance than upper or lower tool radius.

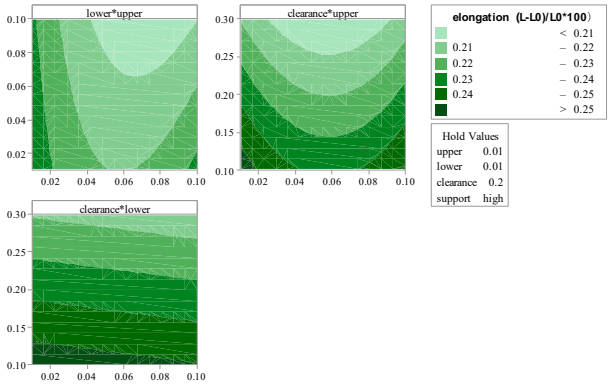


(a)

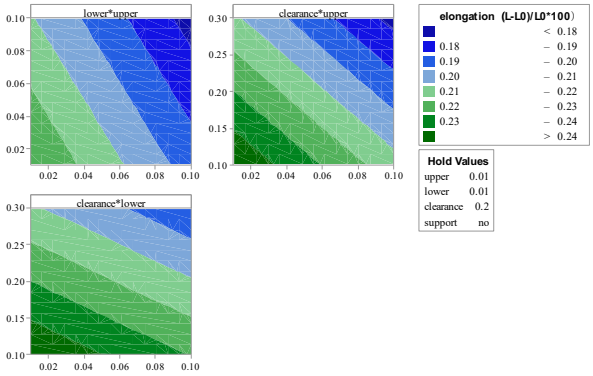


(b)

Figure 2.16: The interaction effect of trimming parameters on total elongation. (a) with support (b) without support

### 2.4.3 Tool sharpness and support selection

To indicate the impact of upper and lower tool sharpness on elongation, figure 2.17(a) and 2.18(b), present the elongation trend and standard deviation. From the upper tool sharpness vs elongation plot, figure 2.17(a), the elongation is less sensitive to the upper tool sharpness for high support. For no support, the elongation is sensitive to the upper tool with a linear decrease trend. In 10% clearance condition, the standard deviation increases with upper tool radius increase. For figure 2.17(b), the elongation is less sensitive to the lower tool radius. The most pronounced decreasing trend was observed at 10% clearance with no-support condition.

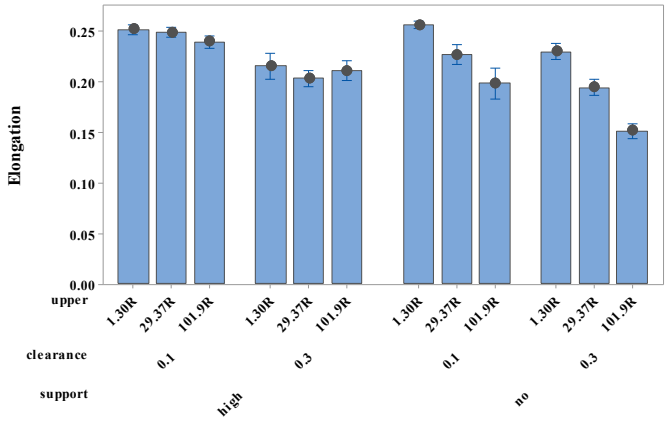


27(a)

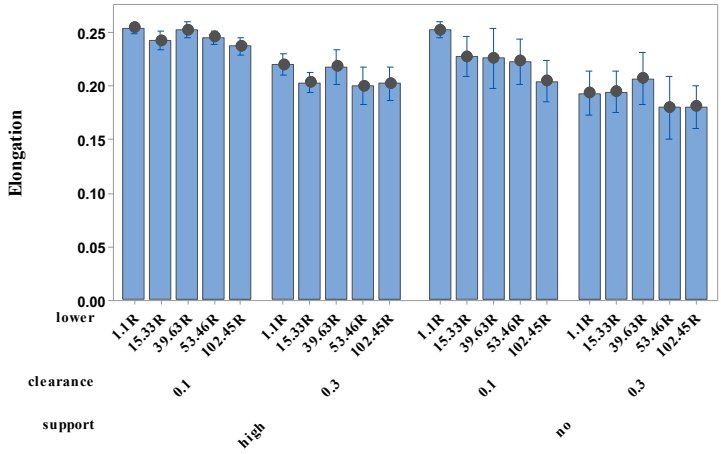


27(b)

Figure 2.17: The effect of tool sharpness on total elongation (a) upper tool sharpness (b) lower tool sharpness

## 2.5 Conclusion

The goal of this chapter is first, to study the effect of multiple trimming conditions on trimmed edge stretchability. Second, find a model correlating the edge stretchability to different trimming conditions and edge geometry parameters. Our findings are summarized as follow:

a. For all investigated trimming parameters, generally, increasing the tool radius and the clearance resulted into a decrease in the elongation. The presence of support leads to a positive effect on the edge stretchability for dull upper tool, while to a negative effect on the edge stretchability for sharp upper tool.

b. The upper tool sharpness has higher sensitivity on total elongation than lower tool sharpness. To reduce the sensitivity of upper tool sharpness on total elongation, the high support introduction is recommended.

c. The rollover and the burr size are a clear indication of the plastic zone extent during trimming and therefore the damage induced to the trimmed edge surface.

d. When the trimmed edge geometry and trimming process parameters are used as explanatory variables, clearance, upper tool radius, burr size, rollover size and burnish size are selected as the most significant variables to predict edge stretchability.

e. The regression model using the trimmed edge geometry parameters as explanatory variables presents better prediction than the one using the trimming process parameters as explanatory variables.

# Chapter 3: Investigation of Alternative Trimming Strategies

## 3.1 Introduction

Automobile industry is attributing to produce fuel-efficient vehicles, which results in the increasing use of the aluminum alloys. A large number of researches focus on tackling aluminum sheet strechability issue. The trimmed edge quality resulted from the trimming process directly influences the strechability and flangeability of the sheared aluminum sheet under stamping. Several shearing strategies have been put forward to improve the sheared edge quality.

In the traditional trimming process, the two surfaces of the tool are perpendicular and the cutting angle, which is the complementary angle of the blade travel direction with respect to the bank, is 0 degree. As an updated strategy to improve the edge quality, Ming Li and Gregory Fata[36] rotated the blank direction and investigated the effect of cutting angle. The shear and normal stress of the surface determined by the cutting angle leaded to worse quality of the steel edge as cutting angle increases. The variation of normal stress changed the aluminum separation mechanism. As a result, the edge quality would first increase and then decrease with cutting angle increases. Li[20] figured out that at appropriate cutting angles, the surface quality became insensitive to the blade sharpness, and almost zero burrs were produced for large clearances and extremely dull blades. Using numerical point-tracking method, S.Senn and M.Liewald[37] investigated that the slant angle, which introduced additional bending and horizontally acting force had a significant negative effect on punch deviation and low effect on punch deflection. Quochung B. Le et al.[24] found that cutting angle expanded the interval of safe FLD-based cutting clearances in his research and correlated cutting angle with failure model by experimental analysis. The angle shearing resulted in two peak loads, lower punch,

lower friction force, also leaded to less tool wear[38]. Jiahui Gu et al.[39] recommended proper clearance value under 2-degree rake angle for AHSS by half dome test. By FE method, Hua-Chu Shih and Guofei Chen[40] investigated the effect of beveled shearing on tool life cycle and crash energy absorption. Shih and Ming[3], [5] put forward a beveled shearing process where the tools with different combination of 3 angles were used to trim the specimens. With the proper combination of angles using tensile and half dome test, the shearing force and energy was reduced and the offal part edge stretch got improved. However, the deficient 3 repetitions increased test deviation. In this study, the clamped aluminum parts trimmed by upper tools with various combination of angles were pulled to failure to estimate the edge stretchability. And the effect of various upper tools on edge stretchability was investigated.

Multiple shearing strategy in the punch process was investigated via collar forming test by Paetzold and M Feistle[6], [41]. In their research, multiple-stage shearing strategy reduced the degree and depth of hardening and eliminated the microscopic damage of steel. The optimal combination of offset and clearance was figured out to maximize forming ability by minimizing work-hardened shear affected zone. Gläsner[42] found that the two-stage shearing process reduced the edge crack sensitivity by reducing the depth of sheared zone. In shaving process, the offset was usually small in order to maximize the proportion of the clean-shear and obtain smooth edge. However, the offset should be larger to achieve a high formability in shaving process[43], [44]. Using punch test, it was hard to vary the offset while keep the other parameters constant in two shearing stages. However, the trimming test can easily fulfill this requirement. In this study, the aluminum edge stretchability under two-stage trimming was estimated by tensile test to investigate the effect of offset on edge stretchability.

This study was the first to investigate the influence of low trimming temperature on the edge stretchability of aluminum. Liquid nitrogen made it possible to trim the materials at a relatively low temperature. Although the aluminum didn't lose ductility with temperature decreases[45], the effect of low trimming temperature on aluminum was also taken into consideration. The room temperature trimmed aluminum edge was set as the baseline of experiment to show the effect of trimming under low temperature.

The objective of this study was to investigate the effect of trimming strategies, such as angle tool trimming, multiple-stage trimming and low temperature trimming, on edge stretchability. Also tried to determine the optimal trimming strategy to improve edge stretchability.

## 3.2 Experimental Technique

The materials used in this experiment were 6DR1 aluminum sheet with 0.9 mm thickness. The materials are widely used for outer vehicle body panels and could be found widely throughout the welding fabrication industry. The specimen geometry used in this study was half dog bone. Two slots paralleling to the specimen main axis guaranteed a trim line which was parallel to the cutting edges. All samples used in this investigation were stored at -50ºC to delay age hardening process. Before trimming the samples were left to warm up at room temperature for 1 hour. After trimming the sample were again stored at -50ºC waiting for the mechanical characterization. The samples were again left to warm up at room temperature for 1 hour before conduction the mechanical characterization. The low temperature storing conditions mentioned above were used to ensure that all samples were tested at the consistent natural age and therefore the results variability induced by age hardening difference was eliminated or reduced.

## 3.3 Test set up and design of experiment

This section introduces the setup of three tests within this study and corresponding DOE. The geometry of upper tool with different rake angles and respective DOE are shown in section 3.3.1. In section 3.3.2, the methods of determining offset values and setting aligned offset are mentioned. Section 3.3.3 shows the method of low temperature trimming and the temperature measurement of trimming point.

### 3.3.1 Angled upper tool trimming test

In this study, the traditional trimming processes with different angle upper tools were investigated. 8 upper tools with different combinations of upper blade rake angle θ1, back cut angle θ2 and shear rake angle θ3 as shown in figure 3.1 were machined. For θ1 and θ2, 0 degree and 10 degree were taken into consideration. 0 and 3 degree were taken into consideration for θ3. The three angles were represented by the format (θ1, θ2, θ3). The

sharpness of all upper tools was confirmed to be similar with 3D optical microscope measurements. The lower tool with 2μm edge radius was utilized in this study. The edge stretchability of 6DR1 aluminum specimens was measured by tensile test. The experiment matrix is shown in table 3.1.

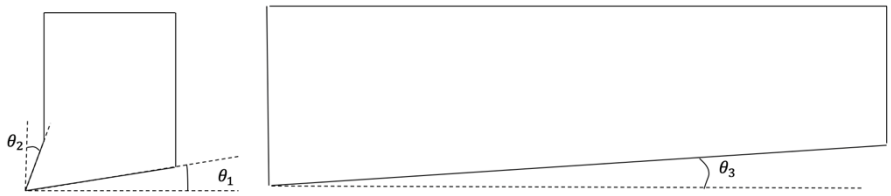


(a) (b)

Figure 3.1: Schematic of upper tool (a) side view of upper tool (b) front view of upper tool

Table 3.1: Experiment matrix of angle trimming

| Parameters | Level |
|---|---|
| Upper tool | (0,0,0), (10,0,0), (0,10,0), (0,0,3), (10,10,0), (10,0,3), (0,10,3), (10,10,3) |
| Lower tool | 2μm radius |
| Clearance | 10% |
| Support | No support |
| Direction | TD |
| Replication | 10 |

### 3.3.2 Two-stage trimming test

The two-stage trimming is defined as the trimming of small cutting-offsets of pre-cut surfaces to produce smooth and dimensionally stable edge[6], as shown in figure 3.2. The trimming conditions of two-stage are same.

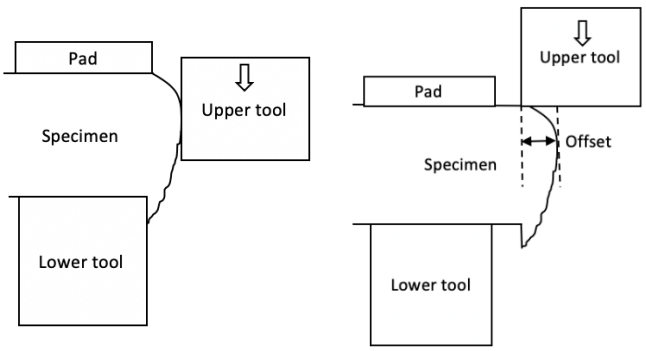


(a) (b)

Figure 3.2: Two-stage trimming strategy. (a) First trimming strategy (2) Second trimming strategy

The goal of this study is to understand the impact of offset on the edge stretchability. To get reasonable offset, the offset was modified until the edge surface with minimum burr size was obtained because the burr size was the major source of early fracture when stretching was applied along the sheared edge. Shims were used to get various offset. As shown in figure 3.3, one side of the shim flushes the back edge of the lower tool. The other side of the shim contacted the specimen. Following this approach, 7 different offsets value were set by using various engage.

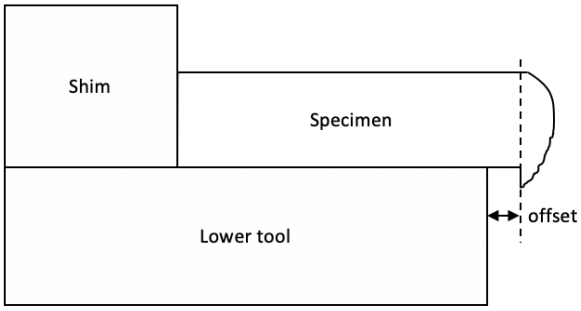


Figure 3.3: Setting offset by engage

Based on the burr size measurement, the offsets of 0.51mm and 2.11mm with minimum burr size were selected. However, the fast and adjustable offset setting method by shim had an alignment problem. The difference between left and right offset could be up to 0.18mm. To avoid this misalignment, new pins were designed as shown in figure 3.4(a) (b). During the experiment, the specimen was aligned using an appropriate pin edge as shown in figure 3.4(c). The difference between left and right offset has been reduced to 0.01mm using this method.

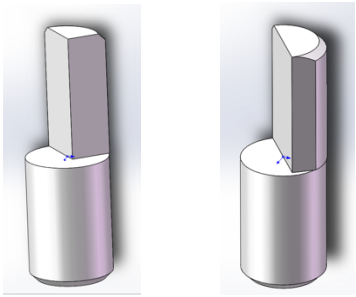

(a) (b)

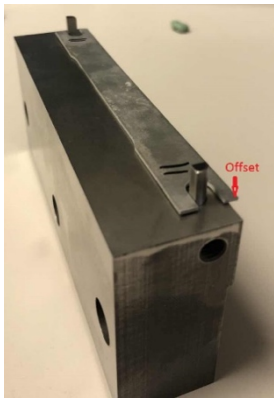


(c)

Figure 3.4: (a) 2.11mm offset pin (b) 0.51mm offset pin (c) setting offset by pins

One-stage trimmed samples with 0.51mm offset pins and 2.11mm offset pins were used as a baseline for comparison. The width of the scrap trimmed using the original pins was 5mm. To simplify the name of the test, the trim step number and corresponding offal part width were used to name the test. For example, the “step1 5mm, step2 0.51mm” meant that the specimen was fist trimmed using the original pins, and then trimmed using 0.51mm pins with a 0.51mm offset. The “step1 5.51mm” meant that the specimen was trimmed using the 0.51mm pins with no subsequent trimming. There were 4 groups sets: “step1 5mm, step2 0.51mm”, “step1 5mm, step2 2.11mm”, “step1 5.51mm” and “step1 7.11mm”. The DOE of the two-stage trimming experiment is shown as table 3.2:

Table 3.2: Experiment matrix of two-stage trimming

| Parameter | level |
|---|---|
| Direction | TD |
| Support | No support |
| Clearance | 30% |
| Upper tool | 2 µm radius |
| lower tool | 2 µm radius |
| Offset | "step1 5mm, step2 0.51mm", "step1 5mm, step2 2.11mm", "step1 5.51mm" and "step1 7.11mm" |
| Replication | 10 |

### 3.3.3 Low temperature trimming test

The liquid nitrogen made it possible to trim the specimen at relatively low temperature. To delay the specimen temperature increase, which took place while it was compressed between the pad and the lower tool, a new thinner G10 pad with lower thermal conductivity (0.288 W/m-K) and shorter compression stroke was utilized as shown in figure 3.5. The thinner G10 pad decreased the trimming temperature significantly and ensured the trimming temperature at reasonable range.

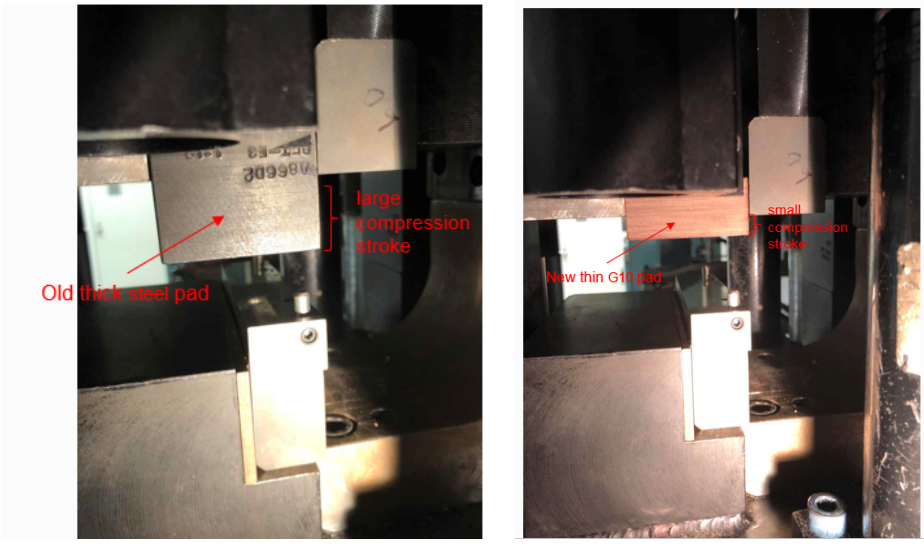


(a) (b)

Figure 3.5: (a) Side view of old thick steel pad (b) Side view of new thin G10 pad

A thermocouple imbedded in the sample connected to a data acquisition module were used to measure the temperature at the moment of fracture during trimming. Two channels as shown in figure 3.6(a) were cut in the specimen to place thermocouple wires making sure the wires

did not disturb the trimming process and implement a good connection of the thermocouple to the specimen. From the temperature history figure, as shown in figure 3.6(c), the process was separated into 3 sections: Before point A, the specimen was in liquid nitrogen keeping the temperature constant; From A to B where the temperature increasing slightly, the specimen was taken out from liquid nitrogen, placed on the lower tool and was raised until it contacts the pad; Increased contact pressure made specimen temperature increase rate significantly higher after point B .

The trimming temperature was identified from the temperature history figure. The time from compression point to trimming point was equal to 1.1s calculated from compression stroke(2.2cm) divided by lower tool close speed(2cm/s) as shown in formula 1. This meant the trimming point was 1.1s after point B. The 6DR1 trimming temperature was -90° C.

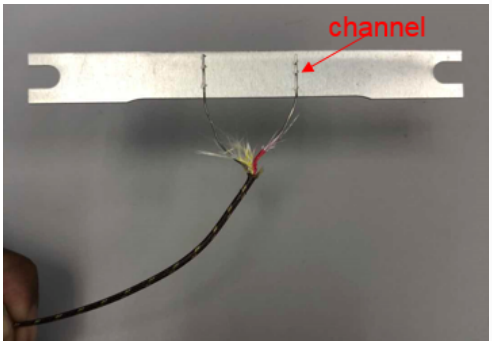


(a)

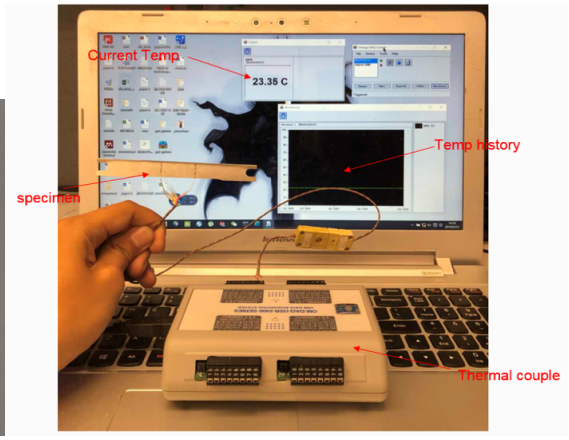


(b)

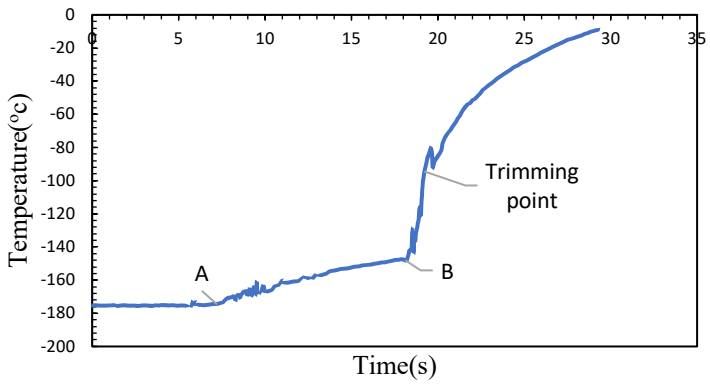


(c)

Figure 3.6: (a) Specimen and thermal couple connection (b) Temperature measurement (c) 6DR1 temperature history

$$\text{Time= compression stroke/trimming speed=1.1s} \quad (1)$$

The trimming conditions were displayed in table 3.3. Two conditions, “sharp upper tool & no support” and “dull upper tool & support” were taken into consideration in DOE because the no support condition resulted in an increase of the edge stretchability when the upper tool was sharp. The upper tools of R200 μm and R2 μm were chosen to represent an extremely dull tool and a sharp tool. The trimming condition at room temperature was also investigated as baseline.

Table 3.3: Experiment matrix of cold trimming

| Parameter | level |
|---|---|
| Direction | TD |
| Upper tool & Support | “R2 μm & no support”, “R200 μm & support” |
| Clearance | 30% |
| lower tool | 2 μm radius |
| Temperature | Room temperature, low temperature |
| Replication | 5 |

## 3.4 Result

### 3.4.1 Determination of the edge stretchability by various upper tools

As was mentioned in above section, 8 upper tools with different geometry were machined in this study. To ensure the results were not impacted by these 8 tools’ sharpness variation, microscopic imaging methods was used to capture actual edge geometry of manufactured trim tools, allowing determination of trim edge radius. For every tool, 3 edge trim edge radius and corresponding standard deviation were measured. From table 3.4, it was clear that 8 tools whose trim edge radius within 10 μm had same edge sharpness. The low standard deviation of measurement showed the consistency of the edge geometry for every tool.

Table 3.4: Tool edge inscribed circle radius and SD

| Upper tool | Average of tool edge radius(μm) | Std Deviation(μm) |
|---|---|---|
| (0,10,0) | 7.23 | 1.72 |
| (10,0,0) | 9.89 | 3.74 |
| (10,10,0) | 6.94 | 2.9 |
| (0,0,3) | 7.54 | 3.25 |
| (0,10,3) | 6.17 | 0.96 |
| (10,0,3) | 8.49 | 2.64 |
| (10,10,3) | 4.94 | 2.84 |
| (0,0,0) | 7.6 | 2.11 |

Trimmed specimens were pulled to failure with the Digital Image Correlation (DIC) tracing the total elongation at break point. The break point was defined as the point where 5% force drop after peak force point in force vs displacement graph. After data collection, one-way ANOVA table was utilized to determine whether there were any statistically significant differences between the means of each group. As a result, p-value equal to 0.462, which indicated the average of 8 groups were equal and the upper tool geometry variety had no effect on the 6DR1 aluminum edge stretch.

Figure 3.7: The total elongation vs upper tools with various shearing rake angles

### 3.4.2 Determination of the edge quality and stretchability by two-stage trimming

The burr, which was the major source of early stretching fracture, was utilized to assess the edge surface quality. The burr size of 7 different offsets for two steps trimmed specimens were measured and shown as interval plot in figure 3.8. The burr size of one-step sample with original pins was set as baseline for comparison and shown by the red lines. From the plot, it was clear that burr size of the two steps trimming sample was much smaller than the burr size of one step trimming sample. The second stage did reduce the edge plasticity area because the previous burr and plastic zone were trimmed off and the offset of the second trimming had no enough material to flow.

187

Figure 3.8: The burr size with various offsets

Trimmed specimens were pulled to failure by a universal tensile machine and the extensometer was used to capture the total elongation at break point. The total elongation of 4 groups were shown in figure 3.9. Based on one-way ANOVA analysis of “step1 5.51mm” and “step1 5mm, step2 0.51mm”, p-value equal to 0.41, which was larger than significant level. This indicated the mean value of two groups were not significantly different and showed that the two-stage trimming with 0.51mm offset had no impact on the edge stretchability. The conclusion was same for the 2.11 mm offset. For the two-stage trimming, the burr size was not a significant parameter to predict edge stretchability. Even though the burr size droped significantly, the edge quality stayed same after second trimming.


Figure 3.9: The total elongation with four different trimming strategies

### 3.4.3 Determination of the cold trimming impact on the edge stretchability

In this study, the tensile test with 2-inch gauge was implemented to assess trimmed edge stretchability with DIC measuring the total elongation at break point. The total elongation under different trimming conditions was shown in figure 3.10. According to the one-way ANOVA table, the “r0.25-cold-high” and “r0.25-RT-high” had same mean value meaning that the low trimming temperature had no effect on the edge stretch for R0.25 upper tool and high support. The same phenomenon also happened with the sharp upper tool and no support trimming condition. All specimens for these four groups fractured at the edge. It was concluded that the low trimming temperature had no effect on the edge stretchability.

Figure 3.10: Elongation data in cold trimming test with different upper tool, trimming temperature and support conditions

## 3.5 Conclusion

The purpose of this chapter is to investigate the influence of multiple trimming strategies, such as low temperature trimming and multiple-stage trimming, on the edge stretchability. Figure out the optimal trimming conditions and strategies. Findings are summarized below:

a. Under 10% clearance, sharp lower tool and no support trimming condition, the multiple rake angles upper tools with similar sharpness had no effect on the edge stretchability.
b. Although the multiple-stage trimming reduced the trimmed edge burr size, the burr size reduction didn't improve edge stretch.
c. For dull tool with support condition and sharp tool without support condition, the low temperature trimming had no effect on the edge stretchability.

# Chapter 4: Conclusion

## 4.1 Summary

The purpose of this study was to investigate the 6DR1 aluminum edge stretch response to variations of the four trimming parameters (clearance, support condition, upper and lower tool sharpness) and trimmed edge geometry parameters (rollover, burnish, fracture, burr and roughness). Three alternative trimming strategies (low temperature trimming, multiple-stage trimming and trimming by upper tools with various rake angles) were also evaluated. The optimal trimming parameters and strategies were determined to maximize sheared edge quality and stretchability. The critical findings are shown below:

a. When the trimmed edge geometry parameters were used as explanatory variables, burr size and rollover size were the most significant variables to predict edge stretchability where the model $R^2$ value reached 77.67%.
b. The tool sharpness had a negative effect on the edge stretchability. The total elongation was more sensitive to the upper tool sharpness than the lower tool sharpness. The high support made edge stretchability less sensitive to the upper tool sharpness.
c. The cold trimming and trimming by various upper tool had no effect on the edge stretchability under designated trimming condition. The multiple-stage trimming led to the burr size reduction, yet had no effect on the edge stretchability.

## 4.2 Limitations

There were several limitations of the methods in this paper. Firstly, only 6DR1 aluminum was used in this study. The finding of this study might not be applicable to other series aluminum or other thickness. Secondly, for low temperature trimming strategies, the location where temperature was measured by thermal couple was not exactly the trimmed area. It was

expected that the temperature in the shear zone was higher due to the heat produced by plastic deformation.

## 4.3 Future work

This study could be repeated and extended to multiple materials and thicknesses. The correlation between trimming cycles and tool wear geometry could be investigated in next step. Determining the wear function of trim tools would be valuable in developing stamping die maintenance schedules, and in specifically determining when tools were outside the optimal parameters. For trimming with multiple new strategies, trimming parameters could be extended to wider range and studied the effect of new strategies on edge stretchability.

# REFERENCES


[1] J. T. Black and R. A. Kohser, *DeGarmo's materials and processes in manufacturing*. John Wiley & Sons, 2017.

[2] K. Lange, "Handbook of metal forming," *McGraw-Hill B. Company, 1985,* p. 1216, 1985.

[3] H.-C. Shih, C.-K. Hsiung, and B. Wendt, "Optimal Production Trimming Process for AHSS Sheared Edge Stretchability Improvement," 2014.

[4] Kalweit, "Edge stretch performance of 6DR1 aluminum in typical automotive blanking conditions," 2017.

[5] H.-C. Shih and M. F. Shi, "Robust Shearing Process for Improving AHSS Sheared Edge Stretchability," in *ASME 2012 International Manufacturing Science and Engineering Conference collocated with the 40th North American Manufacturing Research Conference and in participation with the International Conference on Tribology Materials and Processing*, 2012, pp. 363–369.

[6] I. Paetzold, M. Feistle, R. Golle, W. Volk, A. Frehn, and R. Ilskens, "Determination of the minimum possible damage due to shear cutting using a multi-stage shear cutting process," in *IOP Conference Series: Materials Science and Engineering*, 2018, vol. 418, no. 1, p. 12070.

[7] E. V Crane, "What happens in shearing metal," *Machinery*, vol. 30, no. 763, pp. 225–230, 1927.

[8] K. Wang, L. Greve, and T. Wierzbicki, "FE simulation of edge fracture considering pre-damage from blanking process," *Int. J. Solids Struct.*, vol. 71, pp. 206–218, 2015.

[9] W. Johnson and R. A. C. Slater, "Paper 5: Further Experiments in Quasi-Static and Dynamic Blanking of Circular Discs from Various Materials," in *Proceedings of the Institution of Mechanical Engineers, Conference Proceedings*, 1965, vol. 180, no. 9, pp. 163–181.

[10] X. H. Hu, K. S. Choi, X. Sun, and S. F. Golovashchenko, "Edge Fracture Prediction of Traditional and Advanced Trimming Processes for AA6111-T4 Sheets," *J. Manuf. Sci. Eng.*, vol. 136, no. 2, p. 21016, 2014.

[11] S. F. Golovashchenko, A. M. Ilinich, N. M. Bessonov, and L. M. Smith, "Analysis of trimming processes for advanced high strength steels," *SAE Int. J. Mater. Manuf.*, vol. 2, no. 1, pp. 487–493, 2009.

[12] R. Hambli, “Design of experiment based analysis for sheet metal blanking processes optimisation,” *Int. J. Adv. Manuf. Technol.*, vol. 19, no. 6, pp. 403–410, 2002.

[13] F. Faura, A. Garcıa, and M. Estrems, “Finite element analysis of optimum clearance in the blanking process,” *J. Mater. Process. Technol.*, vol. 80, pp. 121–125, 1998.

[14] S. F. Golovashchenko, “Numerical and Experimental Analysis of the Tirmming Process,” in *Numisheet*, 1999, vol. 99, p. 13.

[15] S. F. Golovashchenko, “A Study on Trimming of Al Alloys Parts,” *Adv. Technol. Plast.*, 1999.

[16] X. H. Hu, X. Sun, and S. F. Golovashchenko, “An integrated finite element-based simulation framework: From hole piercing to hole expansion,” *Finite Elem. Anal. Des.*, vol. 109, pp. 1–13, 2016.

[17] M. Li, “Experimental investigation on cut surface and burr in trimming aluminum autobody sheet,” *Int. J. Mech. Sci.*, vol. 42, no. 5, pp. 889–906, 2000.

[18] G. Fata, “SAE TECHNICAL Sliver Reduction in Trimming Aluminum Autobody Sheet,” no. 724, 1999.

[19] S. F. G. Ã, “A study on trimming of aluminum autobody sheet and development of a new robust process eliminating burrs and slivers,” vol. 48, pp. 1384–1400, 2006.

[20] M. Li, “An experimental investigation on cut surface and burr in trimming aluminum autobody sheet,” *Int. J. Mech. Sci.*, vol. 42, no. 5, pp. 889–906, 2000.

[21] S. F. Golovashchenko, “Analysis of trimming of aluminum closure panels,” *J. Mater. Eng. Perform.*, vol. 16, no. 2, pp. 213–219, 2007.

[22] S. F. Golovashchenko and A. M. Ilinich, “Analysis of Trimming Processes for Advanced High Strength Steels,” *SAE Int. J. Mater. Manuf.*, vol. 1, no. 1, pp. 2008-01-1446, 2008.

[23] S. F. Golovashchenko, “Quality of trimming and its effect on stretch flanging of automotive panels,” *J. Mater. Eng. Perform.*, vol. 17, no. 3, pp. 316–325, 2008.

[24] Q. B. Le, J. A. Devries, S. F. Golovashchenko, and J. J. F. Bonnen, “Analysis of sheared edge formability of aluminum,” *J. Mater. Process. Technol.*, vol. 214, no. 4, pp. 876–891, 2014.

[25] N. Wang and S. F. Golovashchenko, “Mechanism of fracture of aluminum blanks subjected to stretching along the sheared edge,” *J. Mater. Process. Technol.*, vol. 233, pp. 142–160, 2016.

[26] S. M. A. Suliman, “An experimental investigation of guillotining of aluminum alloy 5005,” *Mater. Manuf. Process.*, vol. 16, no. 5, pp. 673–689, 2001.

[27] T. B. Hilditch and P. D. Hodgson, “Development of the sheared edge in the trimming of steel and light metal sheet: part 1—experimental observations,” *J. Mater. Process. Technol.*, vol. 169, no. 2, pp. 184–191, 2005.

[28] E. Gustafsson, *Experiments on Sheet Metal Shearing*. 2013.

[29] T. Universiteit, E. Doi, and D. Version, *Numerical modelling of ductile fracture in blanking*, no. 1999. 2019.

[30] C. Hubert, L. Dubar, M. Dubar, and A. Dubois, “Finite element simulation of the edge-trimming/cold rolling sequence: analysis of edge cracking,” *J. Mater. Process. Technol.*, vol. 212, no. 5, pp. 1049–1060, 2012.

[31] N. S. Manufacturing, “Processing Technology Material fracture and burr formation in blanking results of FEM . simulations and comparison with experiments,” 1996.

[32] S. Shankar, M. Babu, S. Berry, M. Ward, and M. Krzyzanowski, “ScienceDirect ScienceDirect Numerical investigation of key stamping process parameters influencing tool stamping life and wear Numerical investigation of key process parameters influencing tool life and wear Costing models for capacity optimization and,” *Procedia Manuf.*, vol. 15, pp. 427–435, 2018.

[33] A. Dorbane, G. Ayoub, B. Mansoor, R. Hamade, G. Kridli, and A. Imad, “Observations of the mechanical response and evolution of damage of AA 6061-T6 under different strain rates and temperatures,” *Mater. Sci. Eng. A*, vol. 624, pp. 239–249, 2015.

[34] C. Ravi and C. Wolverton, “First-principles study of crystal structure and stability of Al–Mg–Si–(Cu) precipitates,” *Acta Mater.*, vol. 52, no. 14, pp. 4213–4227, 2004.

[35] X. Wu, H. Bahmanpour, and K. Schmid, “Characterization of mechanically sheared edges of dual phase steels,” *J. Mater. Process. Technol.*, vol. 212, no. 6, pp. 1209–1224, 2012.

[36] M. Li and G. Fata, “Sliver reduction in trimming aluminum autobody sheet,” SAE Technical Paper, 1999.

[37] S. Senn and M. Liewald, “Numerical investigation of piercing of DP600 within a critical range of slant angle.”

[38] U. States, S. Corp, H. Shih, D. Zhou, and B. Konopinski, “Effects of Punch Configuration on the AHSS Edge Stretchability,” 2017.

[39] J. Gu, H. S. United, S. Steel, and J. D. Honda, “Effects of Blanking Conditions to Edge Cracking in Stamping of Advanced-High Strength Steels (AHSS),” pp. 1–8, 2018.

[40] H. Shih, G. Chen, U. States, and S. Corporation, “Effects of AHSS Sheared Edge Conditions on Crash Energy Absorption in Component Bend Test,” pp. 1–9, 2018.

[41] M. Feistle, I. Pätzold, R. Golle, W. Volk, A. Frehn, and R. Ilskens, “Maximizing the Expansion Ratio through Multi-stage Shear-cutting Process during Collar Forming,” in *IOP Conference Series: Materials Science and Engineering*, 2018, vol. 418, no. 1, p. 12071.

[42] T. Gläsner, “Reduzierung der Kantenrissempfindlichkeit von Mehrphasenstählen durch 2-stufiges Scherschneiden.” Technische Universität München, 2017.

[43] F. D. Jones, *Die making and die design*. Machinery Publishing Company, 1915.

[44] E. V. Crane, *Plastic working of metals and non-metallic materials in presses*. John Wiley & Sons, 1944.

[45] C. F. Hickey Jr, “Mechanical properties of titanium and aluminum alloys at cryogenic temperatures,” WATERTOWN ARSENAL LABS MA, 1962.